PD INC. physical dynamics, inc.

PD-NW-81-261R

Final Report

30 November 1981

GEOPHYSICAL ANALYSIS OF COHERENT SATELLITE SCINTILLATION DATA

By

E. J. Fremouw

J. M. Lansinger

D. A. Miller

Prepared for

Air Force Office of Scientific Research

Bolling AFB, D.C. 20332

Contract No. F49620-78-C-0014

PD-NW-81-261R

Final Report

30 November 1981

GEOPHYSICAL ANALYSIS OF COHERENT SATELLITE SCINTILLATION DATA

By

E. J. Fremouw

J. M. Lansinger

D. A. Miller

Prepared for

Air Force Office of Scientific Research

Bolling AFB, D.C. 20332

Contract No. F49620-78-C-0014

UNCLASSIFIED

SECURITY CLASSIFICATION OF THIS PAGE (When Data Entered)

REPORT DOCUMENTATION PAGE	READ INSTRUCTIONS BEFORE COMPLETING FORM
1. REPORT NUMBER AFOSR-TR- 82-0012	2. GOVT ACCESSION NO. AD A110773
3. RECIPIENT'S CATALOG NUMBER	
4. TITLE (and Subtitle) Geophysical Analysis of Coherent Satellite Scintillation Data	5. TYPE OF REPORT & PERIOD COVERED Final Technical Report
6. PERFORMING ORG. REPORT NUMBER	
7. AUTHOR(s) E. J. Fremouw, J. M. Lansinger, D. A. Miller	8. CONTRACT OR GRANT NUMBER(s) F49620-78-C-0014
9. PERFORMING ORGANIZATION NAME AND ADDRESS Physical Dynamics, Inc. 300-120th Ave. N.E. Bellevue, Washington 98009	10. PROGRAM ELEMENT, PROJECT, TASK AREA & WORK UNIT NUMBERS 61102F 3210-A2
11. CONTROLLING OFFICE NAME AND ADDRESS AFOSR/NC Building 410 Bolling AFB, D.C. 20332	12. REPORT DATE 30 November 1981
	13. NUMBER OF PAGES 58
14. MONITORING AGENCY NAME & ADDRESS(if different from Controlling Office)	15. SECURITY CLASS. (of this report) UNCLASSIFIED
	15a. DECLASSIFICATION/DOWNGRADING SCHEDULE

16. DISTRIBUTION STATEMENT (of this Report)

Approved for public release; distribution unlimited.

17. DISTRIBUTION STATEMENT (of the abstract entered in Block 20, if different from Report)

18. SUPPLEMENTARY NOTES

19. KEY WORDS (Continue on reverse side if necessary and identify by block number)

Ionospheric scintillation, Phase scintillation, Auroral ionosphere, Ionospheric irregularities, Transionospheric radio propagation.

20. ABSTRACT (Continue on reverse side if necessary and identify by block number)

In May of 1976, Air Force Satellite P76-5 was launched with the Defense Nuclear Agency's Wideband beacon, DNA-002, as its sole payload. Several researchers have employed the resulting data in studies of ionospheric structure and its effect on transionospheric radio communications. In the present work, recordings of amplitude and phase scintillation imposed on Wideband's VHF and UHF signals by the ionosphere

DD FORM 1 JAN 73 1473

UNCLASSIFIED

SECURITY CLASSIFICATION OF THIS PAGE (When Data Entered)

have been used to study medium-scale structures in the auroral-zone F layer. Results include quantitative identification of a very close relationship between scintillation and solar/geomagnetic activity, together with lack of a seasonal variation in scintillation activity in the Alaskan sector. A surprisingly high correlation (90%) was found between monthly means of phase-scintillation index, on the one hand, and sunspot number and 10-cm solar radio flux, on the other. The high-latitude scintillation boundary was found to be very similar to the soft-electron precipitation boundary, including similarity in expansion rates with increasing magnetic activity. Interestingly, it is systematically shifted poleward of the precipitation boundary on the day side of the earth and equatorward on the night side.

The plasma-density irregularities responsible for scintillation were found to be axially symmetric except poleward of the scintillation boundary on the night side. There they exhibit characteristics of sheetlike structures layered like onion skins along magnetic L shells, but recent investigation raises questions about details of this behavior. Specifically, one aspect of the data suggests that the sheetlike configuration may be restricted to the larger-scale end of the spectrum of scintillation-producing irregularities (several km in latitudinal extent).

Taken together, the results of this research disclose a rather direct relationship between scintillation and soft-electron precipitation, with plasma convection likely playing an important role in generation of the scintillation-producing irregularities.

TABLE OF CONTENTS

LIST OF ILLUSTRATIONS

I. INTRODUCTION

A. Background

Various military and civilian systems for communication and navigation, as well as surveillance and tracking radars, depend upon radiowave propagation through the ionosphere, and several must operate in locations where their lines of sight traverse the northern auroral oval and/or the region of structured ionospheric plasma equatorward of it. Thus, increased understanding of the structure and dynamics of the auroral and subauroral ionosphere is a continuing goal of basic research undertaken by Air Force laboratories and Air Force contractors.

This document is the final report on a research project directed at extending knowledge about medium-scale (tens of meters to tens of kilometers) ionospheric structure, which is particularly relevant to transionospheric radio propagation. All such structure, the spatial spectrum of which is strongest at its large-scale end, modulates the phase of signals propagated through it. In addition, irregular structure in the smaller-scale portion of this spectrum results in intensity modulation of radio and radar signals, by means of Fresnel diffraction and often by means of geometrical-optics focusing and defocusing as well.

The complex-signal scintillations represented by the amplitude and phase modulation are of concern for systems operation, but they also provide a tool for describing the scintillation phenomenon and for studying the ionospheric irregularities that produce it. Air Force Satellite P76-5 was launched in 1976 specifically to carry a Defense Nuclear Agency multi-frequency coherent beacon, DNA-002, on a mission to provide information about ionospheric scintillation. This project has involved geophysical analysis of data from P76-5 recorded at Poker Flat, Alaska, in the auroral zone.

B. Research Objectives

The overall objective of this research was to extend knowledge about the occurrence, strength -- and especially the shape -- of ionospheric irregularities that produce radiowave scintillation in the auroral and sub-auroral latitude regimes.

Scintillation data from recordings of the phase of the DNA (Wideband) beacon signals were used to estimate shape parameters and to map out height-integrated irregularity strength. The phase measurements were supplemented, when appropriate, by intensity scintillation data to elucidate propagation aspects of scintillation development, in particular the control of scintillation characteristics by irregularity shape.

The foregoing overall objective comprised several specific aspects. They included exploration of questions regarding the occurrence and strength of the irregularities, such as the presence or absence of seasonal variation and the prominence of a long-term trend tied to the solar-activity cycle. The relationship between irregularity occurrence and other high-latitude geophysical phenomena, such as soft-electron precipitation, also was probed. Special attention was given to identifying occurrence domains (in time and space) of sheetlike and rodlike plasma-density structures. This topic is thought to be particularly germane to identification of irregularity source mechanisms, and it clearly affects the observing-geometry dependence of the transionospheric communication channel.

A more recent specific objective has been critical evaluation of the analysis methods used in this and related work, as well as the assumptions on which they are based. The results of that evaluation have been two-fold: (1) reprocessing of some data, which affected some quantitative results but which did not change qualitative conclusions, and (2) identification of an open question regarding the main high-latitude result of the Wideband satellite experiment.

II. SUMMARY OF THE RESEARCH

A. Theory Employed

The topic of wave propagation in a random medium is a difficult one to treat generally and quantitatively, and it has been approached theoretically from several perspectives (e.g., Ishimaru, 1975). Application of the various theoretical approaches to the subject of transionospheric scintillation has been reviewed recently by Yeh and Liu (1981). There is a consensus in the relevant literature that the relatively simple "phase-screen" approach first proposed by Booker, Ratcliffe, and Shinn (1950) is a broadly useful one.

Current knowledge about the ionosphere is consistent with a characterization of its medium-scale spectrum, in statistical terms, by means of a power-law spatial spectrum (e.g., Fejer and Kelley, 1980), although the statistics may be only locally stationary. Within regions of local stationarity, it appears that the outer scale representing the low-frequency cutoff of the spatial spectrum is very large -- certainly large compared with the processing window effectively employed in the Wideband satellite experiment (Fremouw *et al*, 1978).

Rino and Fremouw (1977) applied phase-screen scattering theory to a random medium made up of ionospheric irregularities characterized by a power-law spectrum, employing a coordinate system conducive to accounting for the effects of three-dimensional anisotropy. Rino (1979a) later specialized the theory to the case of an effectively infinite outer scale and extended it (Rino, 1979b) to the difficult problem of describing intensity scintillation in the presence of multiple scattering. For our phase-scintillation analyses, we have exploited the former (single-scatter) theory to investigate various aspects of irregularity shape (including that of three-dimensionally anisotropic structures) and strength. We restate the directly relevant aspects of the theory here for completeness.

There is experimental evidence that the statistics of phase usually are altered little during propagation of a radio wave between the ionosphere and the ground (Fremouw *et al*, 1978, Livingston *et al*, 1981). Accordingly, to a good approximation, the spatial autocorrelation function, $R_\phi(\vec{\Delta\rho})$, of phase on the ground may be taken as that calculated on the output plane.* Thus

*This identity is exact for the wave's mutual coherence function.

$$R_{\phi}(\vec{\Delta\rho}) = r_e^2 \lambda^2 \ell \sec^2\theta \int_{-\infty}^{\infty} R_{\Delta N}(\Delta\rho + \eta \hat{h} \tan\theta, \eta)\, d\eta \qquad (1)$$

where r_e is the classical electron radius,

λ is the radio wavelength,

ℓ is the thickness of the irregular layer,

θ is the incidence angle on the layer, and

$R_{\Delta N}(\vec{\Delta\rho}, \Delta z)$ is the three-dimensional autocorrelation function of the spatially varying electron density, N. Coupling between the lag dimensions for off-vertical incidence is accounted for by the tan θ term in the argument of $R_{\Delta N}$ when the vertical integration is carried out; $\hat{h}$ is a unit vector along the horizontal projection of the radio propagation vector.

Equation (1) can be sampled directly by means of coherent spaced receivers. The same information is contained in the two-dimensional spatial spectrum, $\Phi(\vec{\kappa})$, which is the following Fourier transform of Equation (1):

$$\Phi_{\phi}(\vec{\kappa}) = r_e^2 \lambda^2 \ell \sec^2\theta \; \Phi_{\Delta N}(\vec{\kappa}, -\vec{\kappa}\cdot\hat{h} \tan\theta) \qquad (2)$$

where $\vec{\kappa}$ is a two-dimensional vector wave number, and $\Phi_{\Delta N}(\vec{\kappa}, \kappa_z)$ is the three-dimensional spatial spectrum of plasma structure.

When a beacon satellite traverses a receiving station, the phase pattern sweeps across the receiving antenna in a direction dictated by the satellite motion. The phase of the received voltage then exhibits a temporal spectrum that depends on the scan velocity and the one-dimensional spatial spectrum described by the integral of Equation (2) over the dimension perpendicular to the sweep. Using a nonisotropic coordinate system introduced by Singleton (1970), one can describe the relevant geometry for scattering irregularities that may be elongated by a factor, a, along the magnetic field and by a factor, b, at right angles to the field in a direction prescribed by an angle, δ, relative to the magnetic L shell. The axial ratios, a and b, are defined relative to the remaining orthogonal dimension (perpendicular to the field line and directed at the angle δ from the magnetic meridian plane).

Upon insertion of a power-law spectrum characterized by a spectral-index parameter, ν, and application of the foregoing geometrical description, Equation (2) becomes

$$\Phi_\phi(\kappa_e) = r_e^2 \lambda^2 \ell \sec^2\theta \, C_s \left(\frac{2}{\alpha^2} + \kappa_e^2\right)^{-(\nu+1/2)} \tag{3}$$

where $$\kappa_e^2 = A\kappa_x^2 + B\kappa_x\kappa_y + C\kappa_y^2 \tag{4}$$

and $$C_s = 4\pi^{3/2} \frac{2^\nu \Gamma(\nu+1/2)}{\Gamma(\nu-1)} \, ab\alpha^{2-2\nu} \left\langle (\Delta N)^2 \right\rangle \tag{5}$$

is the strength (i.e., spectral density) of the three-dimensional spatial spectrum of N at a nonisotropic wavenumber of unity (i.e., 1 rad/m). Normalization is carried out such that the integral over the three-dimensional spectrum equals $\left\langle (\Delta N)^2 \right\rangle$, the variance of plasma density. In Equation (4), A, B, and C are geometrical quantities depending upon the shape of the irregularities through a, b, and δ, and on the observing geometry through the incidence angle, θ, and the geomagnetic heading, φ, of the radiowave propagation vector.

Introducing the satellite motion into the geometrical consideration and performing the relevant integration of Equation (3), one finds that the temporal spectrum of phase is

$$P_\phi(f) = r_e^2 \lambda^2 \frac{\ell \sec^2\theta}{\left[AC - \frac{B^2}{4}\right]^{1/2}} \, C_s \frac{\Gamma(\nu)}{\Gamma(\nu+1/2) V_e} \left[\frac{2}{\alpha^2} + \left(\frac{2\pi f}{V_e}\right)^2\right]^{-\nu} \tag{6}$$

where the effective scan velocity (i.e., the speed with which contours of equal spatial correlation are crossed) is $V_e(A,B,C)$.

Now, the outer scale of ionospheric structure is so large (and possibly ill-defined statistically for a given satellite pass) that the Fourier frequencies, f, actually contained in the spectrum passing through data processing are such that $\sqrt{2\pi} f/V_e >> \alpha^{-1}$. Thus, the spectrum retained may be written as

$$P_\phi(f) = \frac{r_e^2 \lambda^2 \Gamma(\nu)}{(2\pi)^{2\nu} \Gamma(\nu+1/2)} \frac{\sec^2\theta}{\left(AC - \frac{B^2}{4}\right)^{1/2} V_e^{(1-2\nu)}} \ell C_s f^{-2\nu} \tag{7a}$$

$$= Tf^{-2\nu} . \tag{7b}$$

Hence, spectral analysis of phase data from P76-5 yields information on the one-dimensional shape of ionospheric irregularities (namely, the spectral-index parameter, ν). Even simpler processing, consisting merely of calculating the variance, σ_ϕ^2, of received phase, yields information on the strength and three-dimensional shape of the irregularities, since the integral of (7) is

$$\sigma_\phi^2 = 2T \int_{f_o}^{\infty} f^{-2\nu} df = \frac{2Tf_o^{(1-2\nu)}}{2\nu - 1} \tag{8a}$$

$$= \frac{2r_e^2 \lambda^2 \Gamma(\nu) f_o^{(-2\nu)}}{(2\nu-1)(2\pi)^{2\nu}\Gamma(\nu+\tfrac{1}{2})} \frac{\sec^2\theta\, V_e^{2\nu-1}}{\left(AC - \frac{B^2}{4}\right)^{\frac{1}{2}}} \ell\, C_s \tag{8b}$$

where f_o is the cutoff frequency of a detrending filter (Fremouw *et al*, 1978).

The upshot of the foregoing development is that the phase variance may be written as the product of three separable factors, as follows.

$$\phi_\phi^2 = \left[C_\phi(\nu)\, f_o^{(1-2\nu)}\right] \left[G V_e^{2\nu-1}\right] \left[\ell C_s\right]. \tag{9}$$

The first factor may be calculated from the cutoff of the processing filter and the spectral index, ν (or from *a-priori* estimate of ν, since it does not vary greatly); the second factor is the only one that depends upon the observing geometry; and the third factor may be regarded as a height-integrated strength of the irregularities.

The geometrical factor depends upon the quantities A, B, and C, which are defined in Equations (41 a, b, and c) of the paper by Rino and Fremouw (1977) and which are rather complicated functions of the geometry. The physical situation described, however, is quite straight forward. First, the effectiveness of the plasma structure in producing phase modulation is enhanced if the radio wave encounters a high degree of coherence in the medium along the propagation direction -- i.e., if the propagation vector is nearly aligned with some elongation axis of the irregularities. This static effect is accounted for by the geometrical enhancement factor, G. Second,

if the line of sight is scanning across irregularities rapidly, more phase-fluctuation energy is contained in the high-pass spectral window employed for data processing. This effect is accounted for by the effective velocity, V_e. Alignment of the line of sight with a long irregularity axis necessarily means that it is scanning across a short axis (and vice versa), so the two effects reinforce one another.

In part due to the reinforcement of the aforesaid static and dynamic effects, phase scintillation is substantially enhanced within a narrow range of angles centered on grazing incidence to elongation axes of the scattering irregularities. In this research, we have exploited this behavior to obtain estimates (albeit possibly limiting ones) of the axial ratios, a and b, and the orientation angle, δ (=0), and to infer the three-dimensional configuration of the irregularities in various time and space domains. Owing to the narrowness of the geometrical enhancement and the separability of the three factors in Equation (9), one also can employ measurements of phase variance to map out the height-integrated irregularity strength, ℓC_s.

Equations (1) through (9) all deal with the phase scintillation imposed by direct spatial modulation of the radio wave as it traverses the structured ionosphere. Numerous authors have dealt with the problem of the development of fluctuation in signal intensity, I, through diffraction in the post-scattering propagation medium, usually employing the following intensity scintillation index defined by Briggs and Parkin (1963):

$$S_4 \triangleq \frac{\left[\langle I^2\rangle - \langle I\rangle^2\right]^{1/2}}{\langle I\rangle} \tag{10}$$

For instance, Rino and Matthews (1978) have put the intensity scintillation index, for small to moderate values, in the following succinct form:

$$S_4^2 = 4C_I(\nu)\,\frac{T}{V_e^{(2\nu-1)}}\,\frac{F}{G}\,Z^{\nu-1/2} \tag{11}$$

where (Fremouw, 1978)

$$C_I(\nu) = \frac{2^{3\nu}\,\pi^2}{-4\sqrt{2/\pi}}\;\frac{\cos\pi\left(\frac{\nu}{2}-1/4\right)}{\Gamma(\nu)\cos(\pi\nu)} \tag{12}$$

and where

$$F = \frac{ab}{\sqrt{A''}\,C''^{\nu}}\ {}_2F_1\left(\tfrac{1}{2}-\nu,\tfrac{1}{2};1;\frac{A''-C''}{A''}\right) \tag{13}$$

and $$Z = \frac{\lambda z \sec\theta}{4\pi} \tag{14}$$

where A" and C" are geometrical parameters derived from A, B, and C by means of a coordinate rotation, ${}_2F_1$ is the Gaussian hypergeometric function, and z is the "reduced height" (including correction for wavefront curvature) of the scattering structure.

For the most part, the analyses carried out in this research made use of σ_ϕ values from the Wideband experiment, although some use was made of S_4 values. In addition, the results of phase spectral analysis from some satellite passes were used; in particular, the power-law index of the observed phase spectrum, $p = 2\nu$.

B. Some Aspects of Data Processing

The data employed in this study were received by Physical Dynamics from SRI International after some data reduction. The records had been detrended in the field to remove variations with Fourier periods longer than ten seconds in the intensity (due mainly to range change and antenna-pattern effects) and in the phase (interpreted as variations in ionospheric total electron content), as described by Fremouw *et al* (1978). The detrended scintillation records were used for calculation of the scintillation indices, S_4 and σ_ϕ, and for spectral analysis. Most of the data received by PD consisted of digital tapes containing the scintillation indices, spectral parameters, and geometrical information.

The overall data-processing procedure employed at PD's Northwest (PDNW) facility was directed toward assembly of a large data base as well as toward convenient display of individual passes. Pass-summary information was output during initial processing at PDNW in tabular and graphical form to aid in data editing and interpretation. The VHF phase and intensity scintillation indices were graphed as functions of time during each pass. For passes of sufficient interest that spectral analysis was performed, the scintillation-index curves were followed by plots of the

phase spectral strength, T, and spectral index, p ($\approx 2\nu$), for VHF and for UHF. If no spectral data were present, the latter plots are replaced with information on the radio-frequency dependence of phase scintillation.

More information, largely involving pass geometry, was output in tabular form. For each twenty-second time interval, the azimuth and elevation of the satellite as seen from the receiver were output, along with information describing the geometry of line-of-sight penetration of the ionosphere. The satellite look angles were followed by the following quantities relating to the E-layer (110-km) penetration point: incidence angle on a horizontal layer, magnetic heading of the propagation vector, angle between the propagation vector and the magnetic field, the geomagnetic L value, and the VHF Fresnel radius. The same five pieces of information were then repeated for the F-layer (350-km) penetration point. When spectral data were present, line-of-sight velocity information needed for calculating V_e also were output.

Each tape received contained data from approximately fifty Wideband satellite passes, corresponding to about a month of observations. The tapes were pre-processed to produce more compact data files stored on compressed summary tapes at PDNW (as backups) and on a dedicated disc for subsequent processing. It is data from this "morphological disc" that were analyzed in the present study of auroral-zone scintillation, largely by means of a data-sorting program, SYNOP.

The heart of the morphological analysis carried out in this project was contained in Program SYNOP, an interactive program designed to read a large data set, either from tape or disc, and to perform data editing and sorting on command from a user terminal. User/analyst decisions included selection of a parameter for morphological study (σ_ϕ, S_4, T, p, or S_4/σ_ϕ), selection of data according to a criterion such as time of day or magnetic activity index (K_p or College K), and election to invoke or ignore data-editorial criteria.

There were two types of data-editorial criteria. First, one could include or exclude the first and last data points from each satellite pass, as a safeguard against contamination by ground reflections. Second, one could include or exclude data points flagged in a pre-processing routine, CULL. CULL set a data-quality code, IREJ, to -1 (reject) if any of the following conditions was encountered: S_4 at VHF or UHF exceeded 1.3; σ_ϕ or S_4 at VHF was less than 0.009; or the ratios of σ_ϕ at VHF, UHF, and L-Band exceeded pre-determined ranges.

It was expected theoretically and verified experimentally that values of S_4 very much in excess of unity (1.3 established empirically) indicated interference, ground reflection, or equipment malfunctions. Sensitivity of the Wideband receiving system was such that measurement of an apparent phase or intensity scintillation index of less than about 0.01 at VHF indicates a dead recording channel. These two facts underlie the first two CULL criteria.

One of the early findings from the Wideband satellite experiment was that the standard deviation of phase scales quite consistently as $\sigma_\phi \propto \lambda$, where λ is the radio wavelength (Fremouw *et al*, 1978), as predicted by the phase-screen theory. Statistically significant departures from this scaling law indicate either unusual diffractive effects or data-processing problems (such as failure of the detrend processor to track 2π crossings in phase at the lower frequencies). Unusual diffraction events are of interest for applications-oriented studies of individual data segments. They are not of direct interest, however, for morphological studies of ionospheric irregularities using a large data base. Thus, the frequency-scaling criterion was employed as another means to identify and exclude VHF data contaminated by interference, hardware malfunction, or limitations of data-processing software.

During the course of our work with the data base, we found an unexpectedly large number of departures from the $\sigma_\phi \propto \lambda$ scaling law. In particular, we found many highly disturbed cases in which the data base showed a substantially weaker or even reversed wavelength dependence. Figure 1 is an example, showing three-frequency data from a pass that occurred on 2 November 1978 when the local K index (College) was 5. The measured standard deviation of L-band phase (bottom graph) shows a substantial amount of scintillation activity. The other three graphs (top) are of the ratios of σ_ϕ measured at the three frequencies (L band = 1239 MHz, UHF = 379 MHz, VHF = 138 MHz) divided by the ratio of the corresponding frequencies. The expected frequency dependence would produce constant values of unity for all three. Thus, two of the curves reveal substantial depletions in the recorded value of VHF activity when the observed L-band phase scintillation was appreciable.

Early observations of the Wideband beacon signals near the geomagnetic equator showed similar departures from the expected frequency dependence, associated with loss of phase coherence across a band of frequencies at UHF (Fremouw *et al*, 1978). It

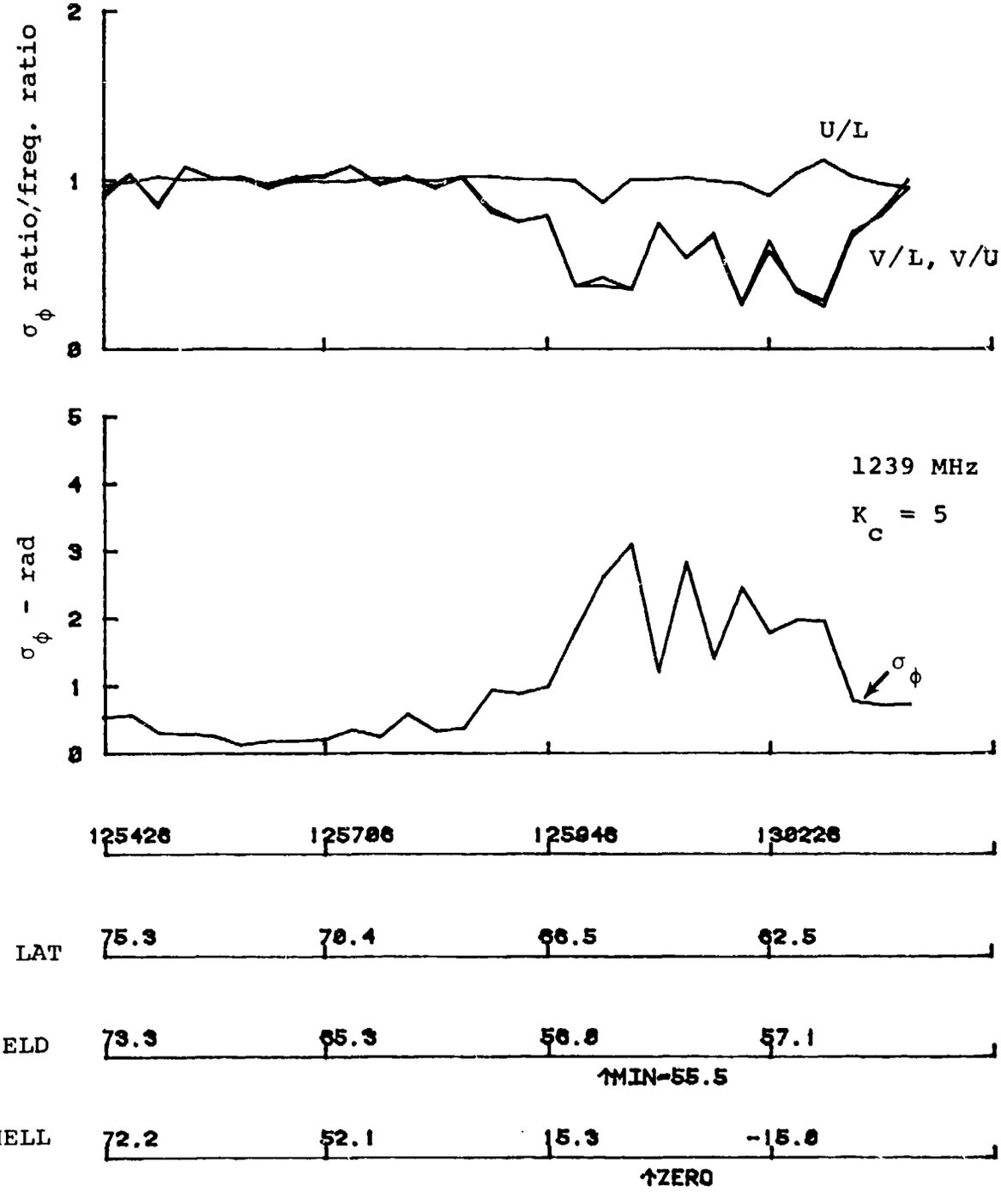

Figure 1. L-band phase scintillation index and ratios of measured to expected frequency dependencies for pass P56-38, which occurred on 2 November 1978.

was found at that time that the extreme phase scintillations sometimes encountered in the equatorial region occasionally were too fast for all 2π ambiguities to be resolved. Only in the present work, however, were such problems noted in the high-latitude Wideband data base.

The rate of change of phase in a given situation decreases with increasing observing frequency (simply because the phase scintillation is less severe). Moreover, the assumptions underlying the simple phase-screen theory, which become increasingly vulnerable as extreme scintillation conditions are approached, are safer the higher the frequency. The simple theory may be used for deducing irregularity characteristics from scintillation measurements so long as a sufficiently high frequency is employed. The lower frequencies, on the other hand, provide greater measurement accuracy under non-extreme conditions.

In view of the foregoing considerations, the final condition flagged by CULL was significant departure from the theoretically expected wavelength dependence of σ_ϕ. From our data base, we could not deduce the precise cause of the departures (e.g. "cycle slipping" in the receivers and/or initial data processing, diffractive invalidation of the simple theory at the lowest frequency, etc.). By making use of the predicted frequency dependence, however, we could cull out those cases in which either equipment or processing problems occurred or the simple theory broke down.

If we had simply excluded from analysis those cases departing from the expected frequency dependence, we would have discarded some of the most interesting cases and biased our data base against highly disturbed conditions. Instead, we employed higher-frequency data when a problem was uncovered, although we employed VHF data in most cases because of its inherent measurement accuracy. Each three-frequency measurement was checked against the expected frequency dependence.

The VHF measurement was compared with those made at UHF and L band, within specified tolerances. If the VHF measured value was too small in both instances or too large in both instances (as could be caused by VHF interference, for instance), it was rejected. Next, UHF was similarly checked against L band and VHF and rejected if too large or too small in both instances. Finally, the L-band measurement was checked against the other two frequencies in the same fashion and rejected if necessary. The lowest retained frequency was employed for analysis,

converted to an equivalent VHF measurement by means of the theoretical frequency dependence.

We applied the foregoing editing procedure to all 35,223 three-frequency measurements in our data population from Poker Flat, each corresponding to a twenty-second period in one of 1043 passes. The VHF measurement of σ_ϕ proved valid in 90.3% of the cases and UHF in another 8.1%. Of the remaining 1.6%, 306 L-band measurements were found valid, and 247 data points were totally rejected.

Once the analyst had made data selections and set editorial criteria, SYNOP performed data sorting and then output the average value of the scintillation parameter being studied (and the number of data points available) in bins corresponding to the following independent variables:

1) Incidence angle, θ, in 1° increments from 0 to 90 ;

2) Off-field angle, ψ_{BP}, in 1° increments from 0 to 90 ;

3) Geomagnetic L at the F-layer penetration point in increments of 1 from 0 to a selectable upper limit;

4) Invariant (geomagnetic) latitude of the penetration point in increments of 1° from 0 to 90° or in increments of 0.1° over a specified range;

5) Geographic latitude and longitude in increments of 1° by 1° over a specified range of latitude and longitude.

6) Angle, ψ_L, between the line of sight and the local L shell in the F layer in 1° increments from -60 to +80°.

The data were output in tabular form and plotted for all bins containing at least three points. For spatial-distribution studies of auroral-zone scintillation, the average index values (multiplied by 100) were output on a grid over ranges of 125° to 168° west longitude and 41° to 80° north latitude. SYNOP also provided the occurrence distribution (cumulative frequency of occurrence vs. observed value) of the selected scintillation parameter. The analysis results, summarized in Section II C, are from the data base collected at Poker Flat between late May of 1976 and February of 1979.

C. Results

We employed the SYNOP outputs in three main studies: trends in the occurrence and strength of auroral-zone scintillation, the three-dimensional configuration (non-

isotropic shape) of the scintillation-producing irregularities, and the location of the irregularities. We report the results of these studies in subsections 1 and 2 of this section. Trends investigated included (a) those with solar activity and related geophysical phenomena and (b) seasonal variation in scintillation strength. As described in subsection 1, the former were found to be rather direct and the later to be nonexistent in the Alaskan sector. We discuss the location and shape of the irregularities together in subsection 2 because the dominant configuration was found to be substantially different in different space-time regions.

1. Trends in Auroral-zone Scintillation

It is generally accepted that high-latitude scintillation increases with solar and geomagnetic activity, based mainly on radiowave amplitude measurements. In this work, the solar and geomagnetic dependences of (primarily) phase scintillation strength at a station in the classical auroral zone (Poker Flat) was investigated. Observational results are presented in this subsection.

Figure 2 simply shows the general increase in phase-scintillation index with local magnetic K index for four years during the advancing phase of the solar cycle. The median and one-radian exceedance values are plotted; viewed in conjunction with Figure 3, these plots afford a general overview of trends in the distribution of phase-scintillation strength in the auroral zone. Figure 3 shows cumulative distributions of VHF phase-scintillation index for the entire 33-month Poker-Flat data base, separately for daytime and nighttime. We have also plotted separately the distributions for measurements made when the radio line of sight was within 10° of grazing incidence on the local magnetic L shell in the F layer. The effect of geometrical enhancement by L-shell-aligned sheetlike irregularities in the nighttime auroral ionosphere is quite evident. We shall return to this effect in Subsection 2.

The secular (year-to-year) trend illustrated in Figure 2 was probed in terms of the relationship of phase scintillation to sunspot number and to 2800-MHz solar flux. Without supposing any direct cause-and-effect relationship between a given solar phenomenon and scintillation, it is still of interest to use an observable such as sunspot number or radio flux as a measure of solar-cycle epoch. In this vein, scatter plots were made of the monthly mean values of σ_ϕ and one-year running averages of spot number and flux, calculated for each month. The scatter plots are shown in Figure 4,

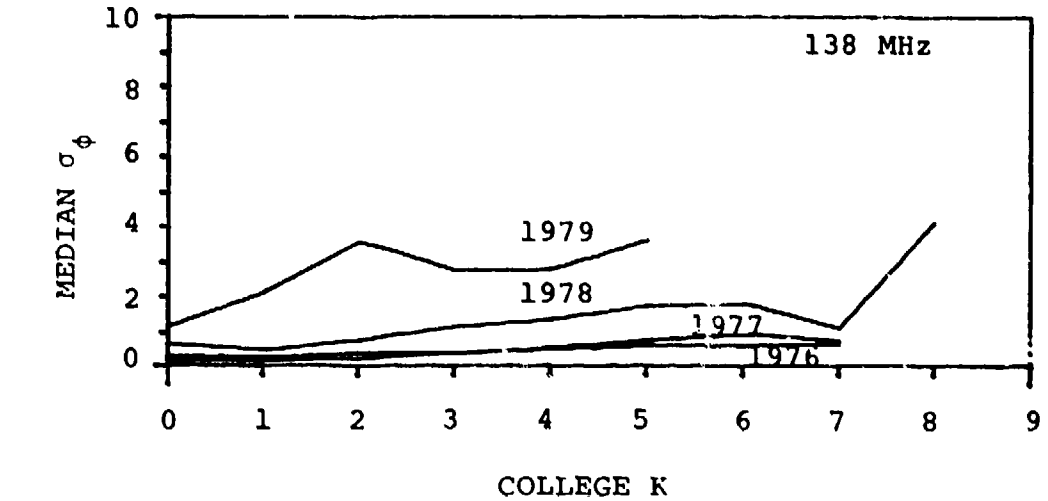

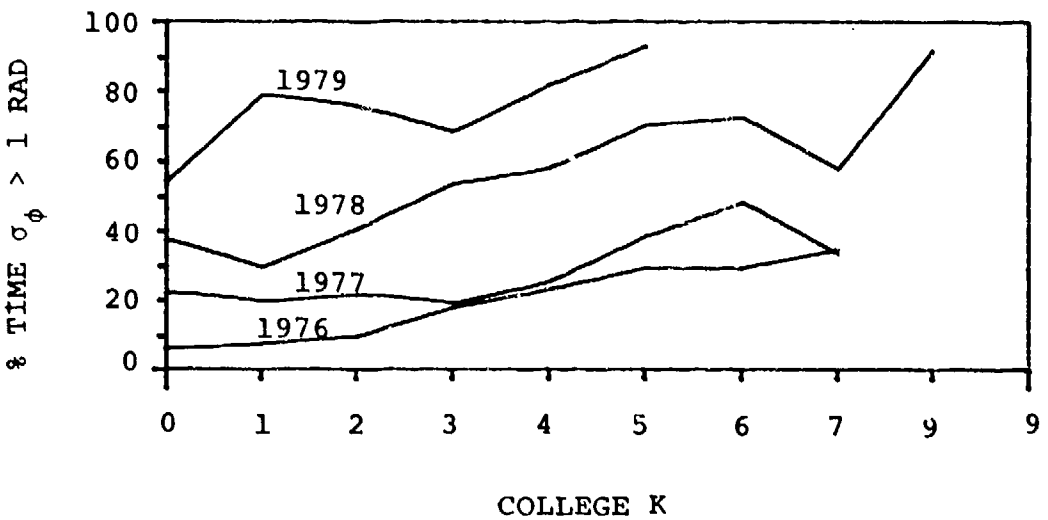

Figure 2. Illustrating general increase in VHF phase-scintillation activity at Poker Flat in years of increasing sunspot number and with increasing geomagnetic disturbance.

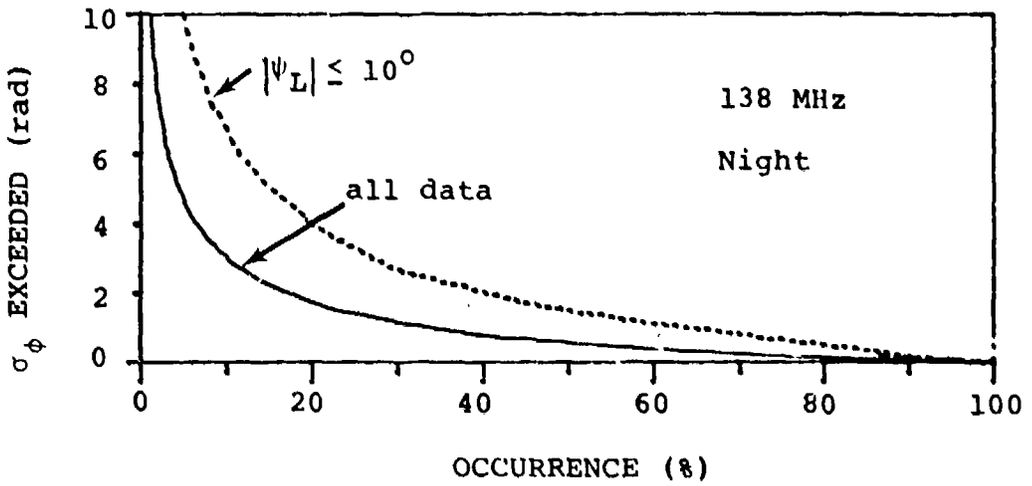

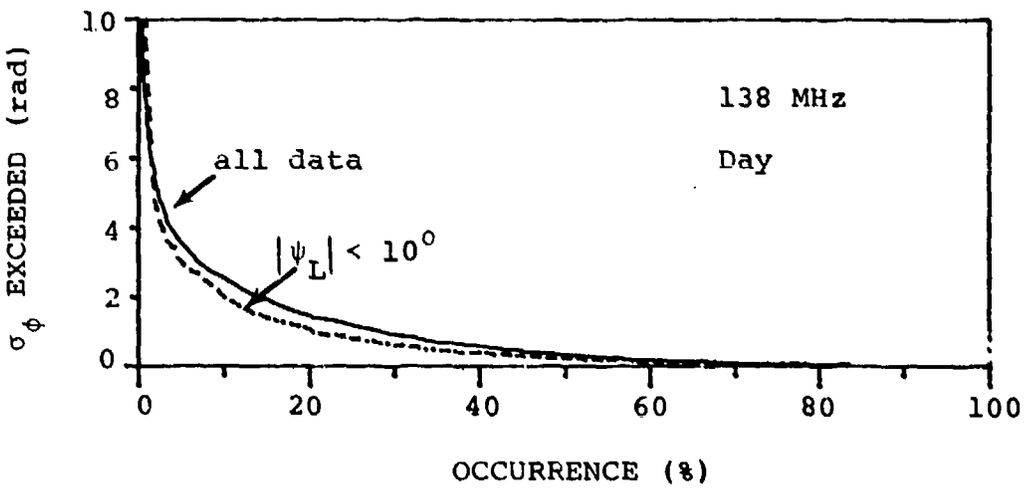

Figure 3. Cumulative distributions of VHF phase-scintillation index at Poker Flat. Abscissa gives percentage of time ordinate value is exceeded. Off-shell angle is designated as ψ_L.

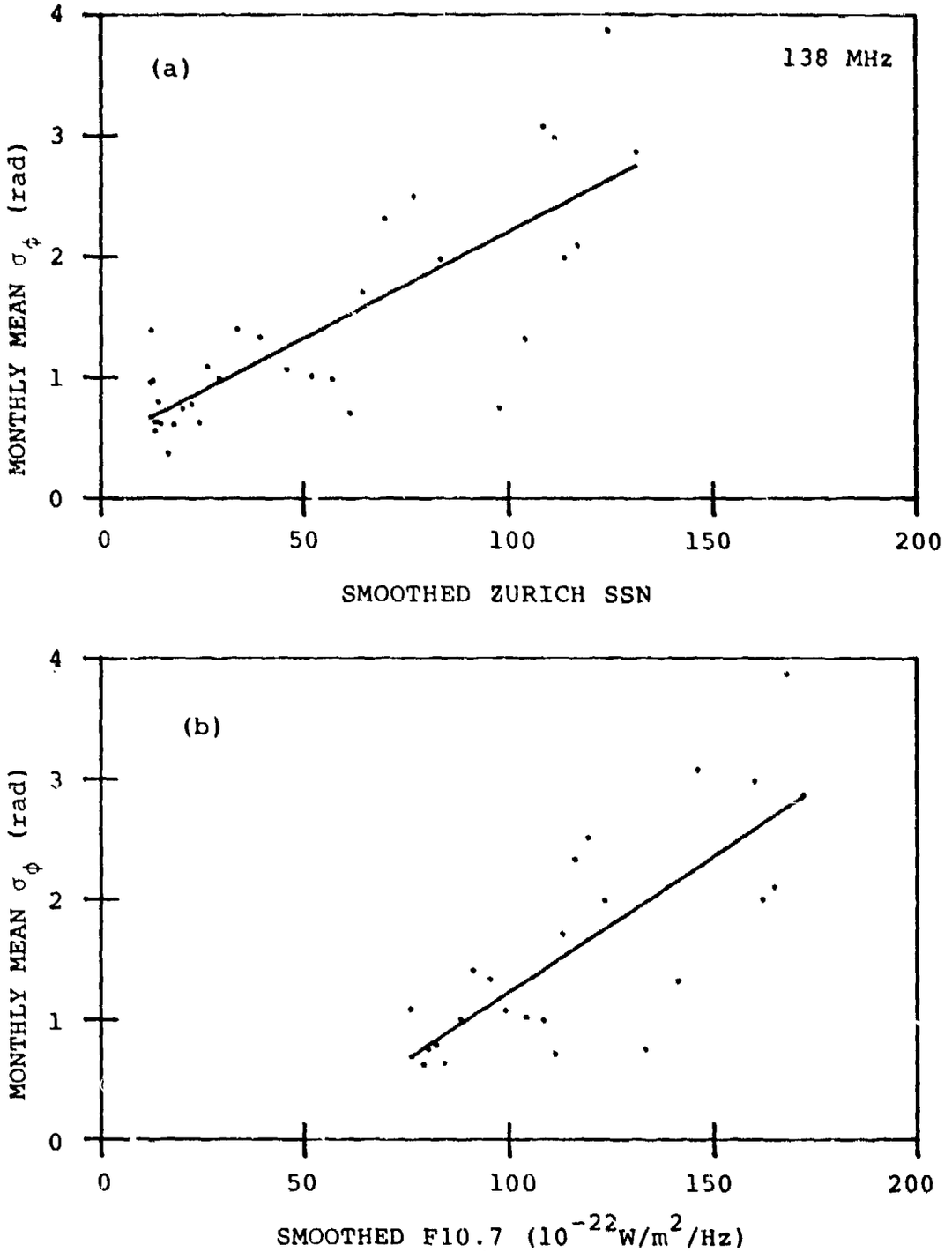

Figure 4. Scatter plots, together with linear regression lines, of monthly mean values of σ_ϕ (20-s rms phase fluctuation levels) at VHF vs. (a) smoothed Zurich sunspot number and (b) smoothed 10.7-cm solar flux. "Smoothed" indicates a one-year running average.

together with linear regression lines showing 78% and 80% correlations of σ_ϕ with (a) sunspot number and (b) solar flux, respectively.

Seemingly of more interest than the correlations is a quasi-cyclic departure of σ_ϕ from both regression lines in Figure 4. One wonders, for instance, whether they might stem from a seasonal dependence of scintillation. The nature of the quasi-cyclic departures is made clear from Figure 5, which contains a scatter plot of monthly mean values of sunspot number against its own one-year running average. The pertinent point is that one finds the same quasi-cyclic departure from the regression line that was demonstrated by the phase-scintillation data. Thus, the departure has to do with variations in solar activity and not with seasonal or other deviations of scintillation production from its ultimate sun-based trigger. Indeed, performing simple linear-regression analyses of monthly mean values of σ_ϕ against monthly mean values of (a) sunspot number and (b) solar flux yields correlation coefficients of 91% and 89%, respectively. The correlation between the two sets of solar data themselves is 98%, which accounts for the close similarity in scintillation correlations relative to the two.

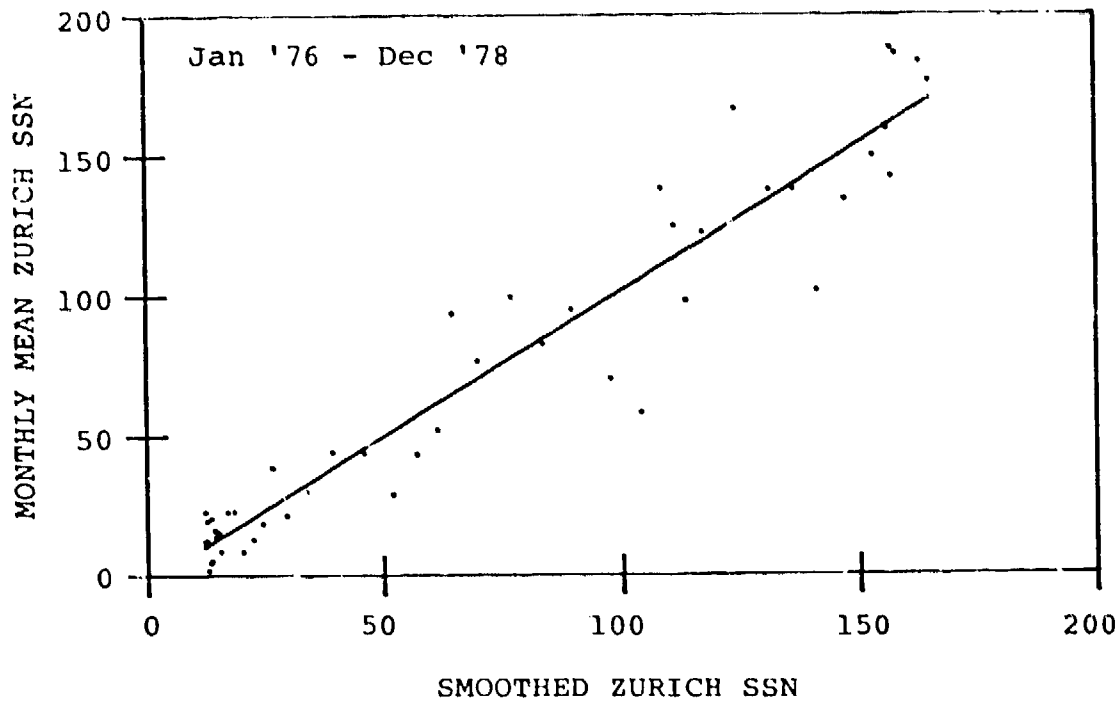

Figure 5. Scatter plot of monthly mean values of Zurich sunspot number vs. one-year running average of the same values. Note quasi-cyclic departure from the regression line, as in Figure 4.

The matter of seasonal variation in scintillation activity is of interest both for geophysical and systems applications. Basu (1975) found a marked seasonal variation in VHF intensity scintillation upon analyzing nighttime recordings of the signal from ATS-3 obtained at Narssarsuaq, Greenland. The most striking feature in her results was a deep and very consistent winter minimum observed in each of four consecutive years (1968 through 1971).

The seasonal variation of nighttime scintillation found by Basu was consistent with enhancement of scintillation activity during times of high-latitude geomagnetic disturbance and with the idea that such disturbance is modulated by the orientation of the magnetosphere relative to the solar equatorial plane in a particular way. Basu found, in the same work, that the negative component, AL, of the auroral electrojet index, AE, displayed the combined seasonal and diurnal variation predicted for auroral particle precipitation on the basis of a model involving Kelvin-Helmholtz (K-H) instability in the flanks of the magnetosphere (Boller and Stolov, 1970). The AL index had been found by Meng and Akasofu (1968) to be a good indicator of particle precipitation in the nighttime (negative-bay) sector of the auroral oval.

Now, AL is a measure of auroral electrojet strength throughout the northern auroral oval, so its diurnal variation is expressed in universal time (UT). It is the difference between UT diurnal variations in summer and winter that Basu took to be related to the seasonal variation of nighttime scintillation that she observed. (See her Figure 2.) At a different longitude, a nighttime phenomenon associated with the auroral electrojet would be expected to show a different degree of seasonal variation. The chain of reasoning predicts little, if any, seasonal variation in scintillation in the local midnight hours in Alaska (where local midnight corresponds to 1000 UT).

To test the foregoing prediction, we selected nighttime data (between 2230 and 0230 local time) for which the F-layer penetration point (at 350 km) was between 64° and 74° geomagnetic latitude (i.e., within the auroral oval but not so far north of the station that the data population became sparse) and grouped them according to season, centered on the soltices and equinoxes. For this data subset, we calculated the mean values of σ_ϕ and S_4 and their percent occurrence above a threshold, for comparison with Basu's results from Greenland. (Her fixed F-layer penetration point was at 64° geomagnetic.)

The results are presented in the table on page 21, along with standard deviations of σ_ϕ and S_4 and the number of data points contained in each of the seasonal data populations. The results also are plotted in Figure 6, the dominant characteristic of which is a roughly three-fold increase in nighttime scintillation activity in the auroral oval during approximately the first quarter of the present solar cycle. There is no semblance in Figure 6 of the summer maximum found by Basu and but a single suggestion (1977) of the consistently deep winter minimum seen in her Figure 3.

The marked difference in seasonal behavior of local-nighttime scintillation observed in Greenland and in Alaska supports the idea of a link between scintillation-producing irregularities in the auroral precipitation zone and the orientation of the magnetosphere relative to the solar wind. Specifically, it is consistent with a prediction stemming from the seasonal-diurnal variation of auroral electrojet activity that itself is based on the considerations by Boller and Stolov (1970) of variations in K-H instability in the flanks of the magnetosphere.

It is argued that a component of the geomagnetic field parallel to the solar wind has a stabilizing influence. Analysis of the K-H instability and the relevant geometry suggests a summertime maximum instability near 0430 UT and a wintertime maximum near 1630 UT, which Basu observed in AL behavior. A seasonal variation in related phenomena should maximize near these times and minimize between them. Basu's scintillation data were obtained between 0100 and 0500 UT, while those shown in Figure 6 are from between 0830 and 1230 UT. Thus, the former data set included a time of maximum predicted seasonal variation, and the latter was centered on a time of minimum predicted seasonal variation; the behaviors are as predicted. We conclude that the lack of a seasonal variation in the nighttime Wideband scintillation data from Poker Flat -- as contrasted with the marked seasonal variation in nighttime ATS scintillation data from Narssarssuaq -- strongly supports a link between high-latitude scintillation and the orientation of the magnetosphere relative to the solar wind.

2. Shape and Location of the Irregularities

The concept of an equatorward boundary of the high-latitude scintillation region (Aarons, Mullen, and Whitney, 1969) is well established on the basis of amplitude observations (Aarons, Mullen and Basu, 1964; Aarons, Silverman and Ramsey, 1966;

TABLE: TABULAR VALUES OF SEASONAL MEASUREMENTS

Season	Number of Observations	$\langle S_4 \rangle$	SD_{S_4}	% Time $S_4 > 0.3$	$\langle \sigma_\phi \rangle$	SD_{σ_ϕ}	% Time $\sigma_\phi > 1$ Rad
76 SU	1251	0.231	0.163	22.54	1.053	1.171	34.29
76 AU	815	0.183	0.134	13.6	0.619	0.716	17.30
76 WI	1488	0.146	0.144	9.54	0.621	0.831	16.53
77 SP	774	0.157	0.133	9.56	0.737	0.973	21.06
77 SU	883	0.218	0.157	20.84	0.942	0.911	31.26
77 AU	1186	0.265	0.183	30.35	1.336	1.422	45.87
77 WI	1319	0.221	0.167	20.39	1.101	1.265	34.27
78 SP	851	0.422	0.256	64.98	2.282	2.153	66.51
78 SU	316	0.357	0.195	54.75	0.915	0.844	63.29
79 AU	766	0.474	0.264	67.75	2.375	2.169	69.06
78 WI	1432	0.435	0.299	55.73	2.495	2.433	67.25

KEY: S_4 = intensity scintillation index

σ_ϕ = phase scintillation index

SD = standard deviation

$\langle\ \rangle$ = mean

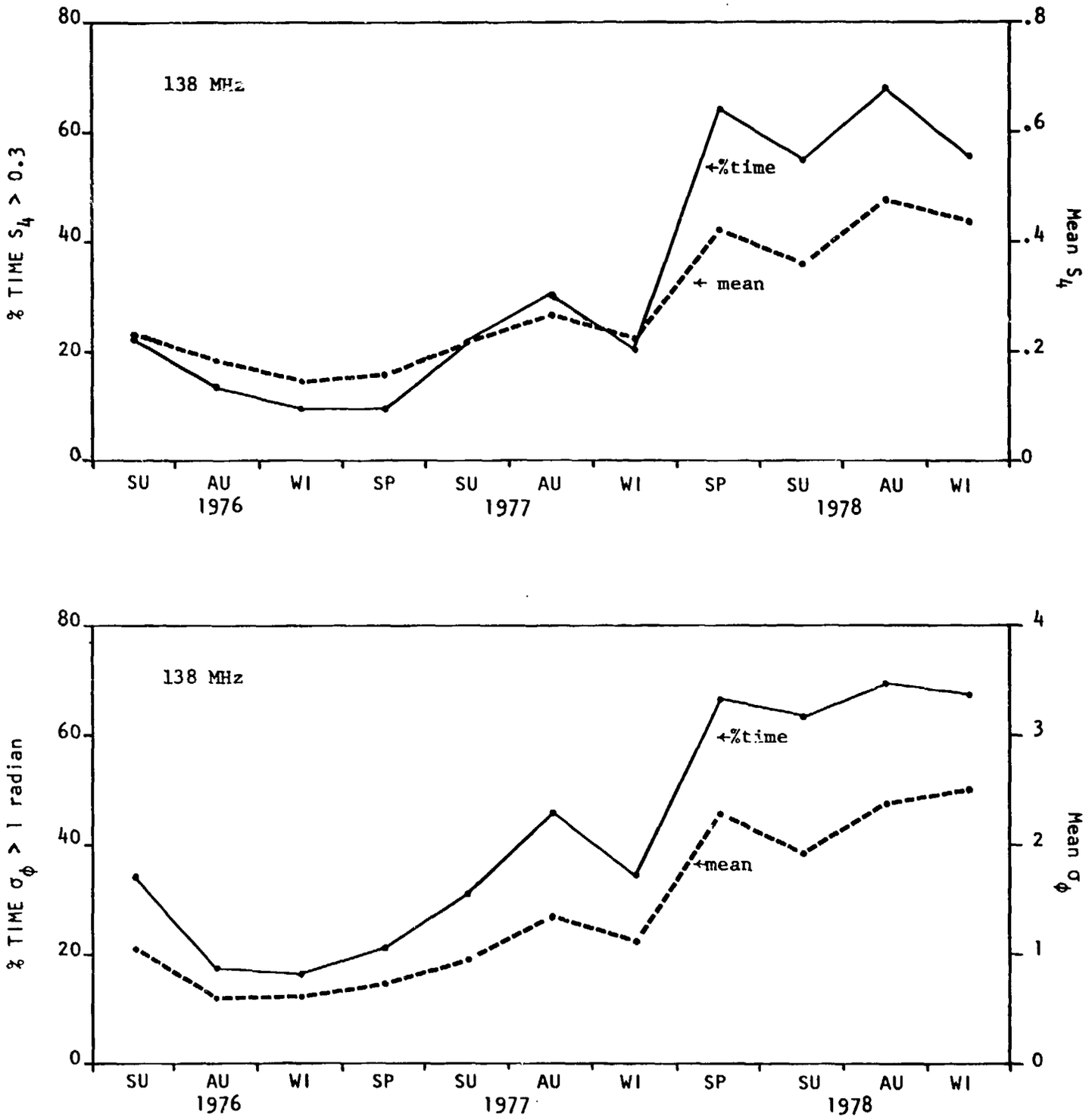

Figure 6. Trends in nighttime phase (bottom) and intensity (top) scintillation strength observed at Poker Flat, Alaska, in the first 2½ years of operation of the Wideband beacon.

Aarons, 1973). Yet, weak scintillation does occur equatorward of the boundary. Given the excellence of the Wideband data base, particularly for phase scintillation, and the strategic location of Poker Flat, we sought to elucidate two aspects of the boundary's nature. First, we sought to quantify the relationship between its location and other high-latitude geophysical phenomena, and second, we determined the dominant shapes of the irregularities just poleward and just equatorward of the boundary on the day and night sides of the earth.

In an annual report on this contract (Fremouw and Lansinger, 1979), we showed preliminary results on the equatorward migration of the dayside scintillation boundary with increasing College K index. It is no surprise that the data -- both dayside and nightside -- from the total collection are well ordered also in planetary geomagnetic index, K_p. We have used the data sorted and analyzed in this research effort as the basis for an applications-oriented scintillation model being developed under separate contract (Fremouw and Lansinger, 1981).

The most concise way to state the analysis result on boundary location is in terms of a simple equation from the model. The equation describes the average invariant latitude of the boundary as a function of time, T_m, after local magnetic midnight and of K_p, as follows:

$$\lambda_b = 71^\circ - 1.5\, K_p - 5.5 \cos \frac{\pi(T_m - 2)}{12} . \qquad (15)$$

Thus, the boundary closely approximates a circle whose center is offset from the magnetic pole by 5.5° toward the day side of the earth and whose quiet-time radius of 19° expands with increasing magnetic disturbance at the rate of 1.5° per unit of K_p. The line of symmetry along which the center is shifted away from the pole is not the noon-midnight meridian, but rather is rotated 2° later in time. The rotation is based on a finding of Basu and Basu (1981) from *in-situ* irregularity data. When it was incorporated into the scintillation model, improved fits to relevant subsets of the Poker Flat data population were achieved.

Figure 7 compares the quiet-time boundary ($K_p = 0$) described by Equation (15) with the quiet-time boundary found by Gussenhoven *et al* (1981) for soft (low end of the 50-ev to 20-kev range) electrons precipitating into the diffuse-auroral ionosphere.

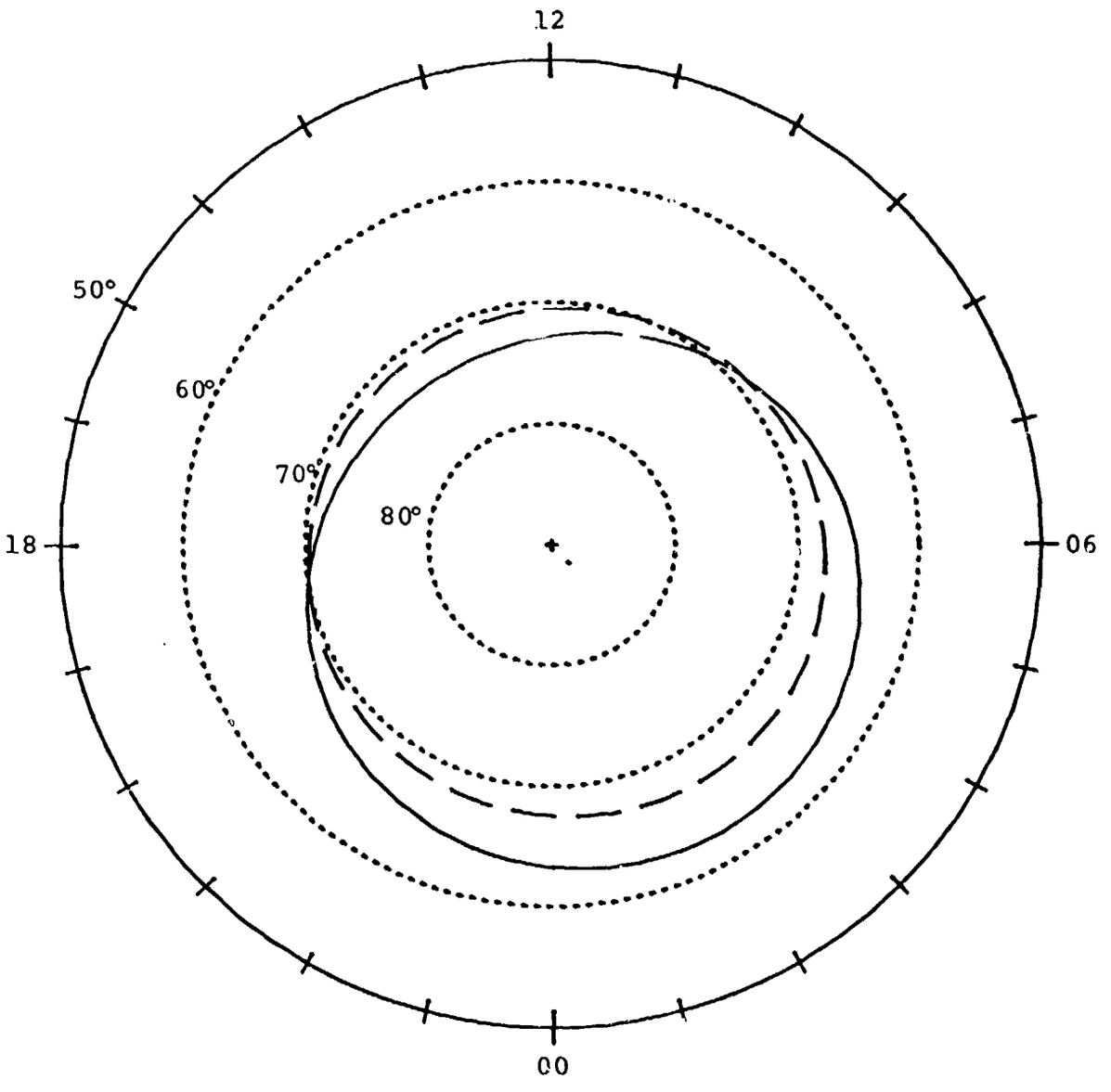

Figure 7. Comparison, in geomagnetic latitude/time coordinates, of the quiet-time scintillation boundary observed at Poker Flat and the quiet-time boundary of soft electron precipitation found by Gussenhoven *et al* (1981). Magnetic-disturbance expansion rate is approximately 1.5° per unit K_p for the former and between 1.2° and 2.2° per unit K_p for the latter.

There are three pertinent similarities and one interesting difference between the two boundaries. The similarities are, first, that they are both essentially circles, which comes as no surprise; second, that their axes of symmetry are both rotated by the same angle from the magnetic noon-midnight meridian; and, third, that their rate of expansion with increasing magnetic activity is essentially the same. The interesting difference is that the scintillation boundary is shifted more toward the night side of the geomagnetic pole than is the precipitation boundary.

The foregoing behavior is consistent with the idea that scintillation-producing irregularities are born of precipitation-produced plasma during the course of its generally anti-sunward convection over the polar cap. The family of convective instabilities that includes the gradient-drift (Linson and Workman, 1970) and current-convective (Ossakow and Chaturvedi, 1979) processes provides viable hypotheses as production mechanisms.

It is likely that three-dimensional irregularity shape will turn out to be important information for sorting out production hypotheses, and *in-situ* measurements cannot provide such information. Doing so is the forte of scintillation observations, especially of phase because of the second factor in brackets in Equation (9). With this in mind, we investigated the dominant configuration of irregularities poleward and equatorward of the scintillation boundary on the day and night sides of the earth. The task was to establish clearly whether irregularities in each of these four regions are isotropic, two-dimensionally anisotropic (aligned like rods along the magnetic field), or three-dimensionally anisotropic (sheetlike, layered like onion skins along magnetic L shells).

Referring again to Equation (9), for isotropic irregularities G goes to unity and V_e reduces to the velocity of the line of sight perpendicular to itself at the ionospheric penetration point (Rino and Fremouw, 1977). For the Wideband viewing geometry from Poker Flat, field-aligned axially symmetric irregularities increase the factor product GV_e^q (where $q = 2\nu - 1$) substantially within a cone of look angles centered on the receiver's magnetic zenith. For L-shell aligned sheetlike irregularities, the enhancement extends along a line of constant L in the scattering layer. Our approach has been simply to identify conditions under which one or the other of these enhancements is present.

We had noticed (Fremouw *et al*, 1978) that scintillation observed at Poker Flat displayed a geometrical enhancement along the local L shell at night but not in the day-time. This behavior, however, could represent simply a difference between the auroral ionosphere and the mid-latitude ionosphere, since the high-latitude precipitation and scintillation boundaries typically are located near or equatorward of the station at night and poleward of it during the day.

In a first attempt to separate latitudinal from diurnal effects, we sorted the daytime data base according to local (College) K index. Results were suggestive but not conclusive. We found that for sufficiently high K, the scintillation boundary usually was equatorward of Poker Flat, and we observed no geometrical enhancement in the corresponding aggregate data. There were too few clearcut cases, however, for definitive conclusions; while the scintillation boundary migrates equatorward with increasing K index, on average, the spread in its location for a given K is considerable. Moreover, a geometrical enhancement due to rodlike irregularities could be masked by such a simple sorting.

As a result of the foregoing, we inspected the entire Poker Flat data base, in the form of pass-summary charts, and manually selected those cases in which a boundary was identifiable. The existence of a scintillation boundary is by no means always clear in individual passes, and its identification is somewhat subjective. What we sought were passes clearly showing two levels of scintillation activity, with scintillation consistently stronger poleward of some transition latitude than equatorward of it. The transition was taken to represent the high-latitude scintillation boundary. We found 98 such daytime passes in which the boundary was equatorward of Poker Flat. They did occur predominantly, but not exclusively, under conditions of elevated K (their average K being 2.32 as compared with 1.84 for the entire daytime data population). Daytime passes occurred between 0600 and 1300 local standard time (150° WMT), and nighttime passes took place between 2100 and 0500.

The satellite is in a sun-synchronous orbit, so we were able to classify pass geometry on the basis of time. Passes suitable for distinguishing between isotropic and field-aligned irregularities are those that come close to the magnetic zenith. For day time and night time respectively, we defined the following pass-time corridors for which the minimum off-field angle of the line of sight was no more than about ten

degrees: 0944-1022 and 0018-0059 local standard time. The latter time window occurred near local magnetic midnight, and passes within that corridor progressed from north to south essentially along the magnetic meridian. Daytime passes were from south to north at a larger angle to the meridian.

Passes for which the minimum off-field angle was large (very much greater than ten degrees) would be expected to produce a geometrical enhancement only for sheetlike irregularities (except for the unlikely case of nonfield-aligned rodlike irregularities). Thus, the existence or absence of an enhancement was noted separately for magnetically "overhead" and "nonoverhead" passes in each of the four latitude/time zones. Recall that the latitude separation was according to whether the scintillation boundary lay poleward or equatorward of the receiving station.

The simplest situation encountered is illustrated in Figure 8, which shows measurement results from a nighttime pass during which the scintillation boundary was poleward of the station. The top panel shows the VHF phase and intensity scintillation indices, σ_ϕ and S_4 respectively, as functions of time and penetration-point geometry. The lower panel shows (in dB relative to 1 rad^2/Hz) the power spectral density (PSD) at a fluctuation frequency of 1 Hz, obtained from spectral analysis of the phase record. The bottom scale denotes the invariant latitude of the line-of-sight penetration point with the F layer (350 km altitude).

A visual scan of any of the three records in Figure 8 shows modest but sustained scintillation activity throughout approximately the northern half of the pass and weaker scintillation at its southern end. The existence of a scintillation trough between the mid-latitude scintillation region (bounded presumably by the plasmapause) and the high-latitude scintillation region is consistently shown. The transition latitude between the trough and the high-latitude region is identified as the scintillation boundary. The station latitude (64.8° invariant) was well inside the trough, in this case.

The upper two scales in the figure show (top) the angle between the line of sight and the magnetic field, which minimized at 39.1° in this nonoverhead pass, and (lower) the angle between the line of sight and the local L shell (both calculated at the F-layer penetration point). In contrast with figures soon to be shown, Figure 8 reveals no prominent feature that could be identified as a geometrical enhancement. Absence of

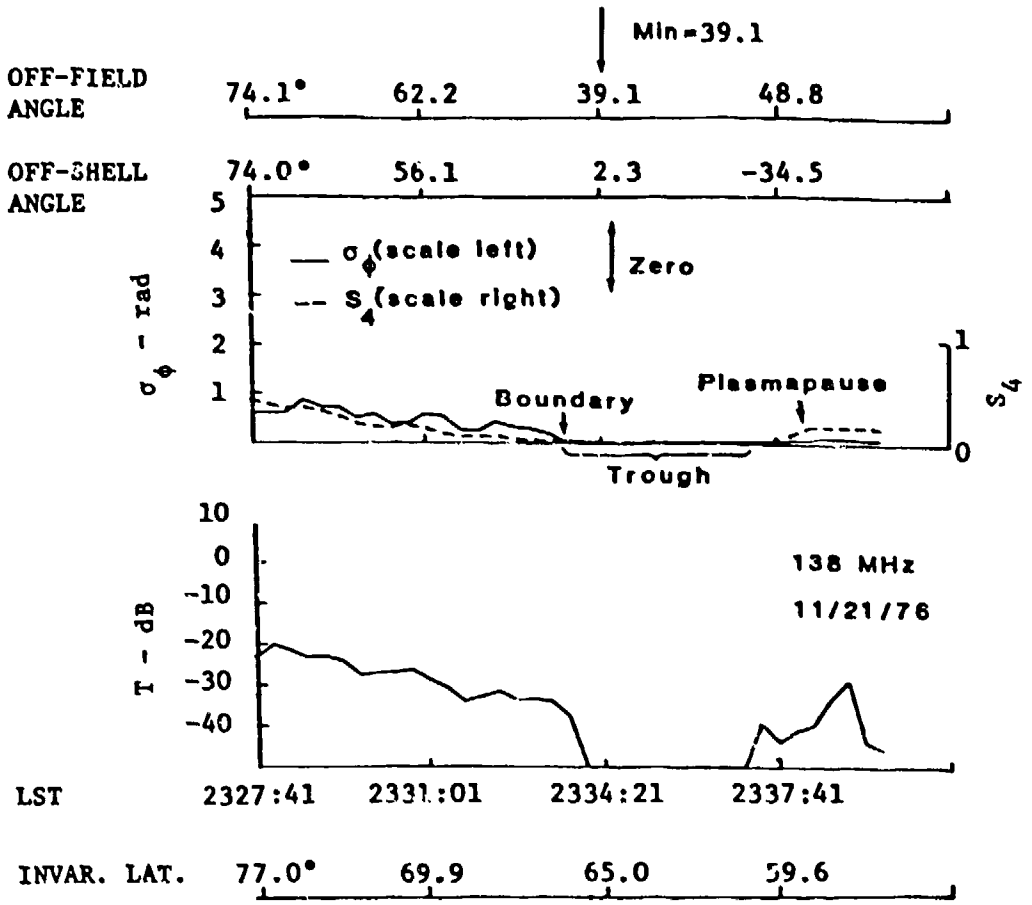

Figure 8. VHF scintillation indices (top) and PSD of phase (bottom) for a nighttime, off-meridian (i.e., nonoverhead) pass during which the scintillation boundary was poleward of the station. Note absence of geometrical enhancement, in contrast to Figure 9.

an enhancement at the zero off-shell point, identified by the double-headed arrow, is a null result (corroborated by other such passes) indicating that there were no L-shell aligned sheetlike irregularities in the trough.

Figure 8, of course, would be equally consistent with the total absence of scintillation-producing irregularities -- of whatever configuration -- in the trough. Figure 9, however, shows the remarkable ability of geometrical enhancement to reveal even weak irregularities. It illustrates measurement results for an overhead nighttime pass in which the trough was equally quiet and, in fact, latitudinally broader than in Figure 8. A very prominent scintillation feature (again corroborated by other passes) occurred as the line of sight made its closest approach (|0.1) to the magnetic zenith, which we interpret as a geometrical enhancement due to field-aligned rodlike irregularities in the trough.

Thus, just as there is a low-density plasma in the main ionospheric trough, so there are weak irregularities in the associated scintillation trough. They are so weak, however, that they often escape detection by scintillation observers unless enhanced by favorable geometry, as in Figure 9. The fact that enhancement is achieved only on passes near the magnetic zenith indicates that these trough irregularities are axially symmetric about the magnetic field.

The markedly different, and by now expected, situation that occurs when the nightside scintillation boundary is equatorward of the station is illustrated in Figure 10, which shows the scintillation indices recorded on (a) a nonoverhead and (b) an overhead pass. In this circumstance, a sharp geometrical enhancement occurs at the zero off-shell point in the nonoverhead case as well as in the overhead one. This oft-repeated behavior is the clear signature of sheetlike irregularities aligned along L shells. That is, the irregularities poleward of the high-latitude scintillation boundary not only are stronger than those in the trough but, in addition, they are three-dimensionally anisotropic.

Daytime passes over Poker Flat progress oppositely to nighttime passes (i.e., from south to north), and Figure 11 illustrates the common daytime situation in which the scintillation boundary is located well north of the station. In the nonoverhead pass illustrated in Figure 11a, there was clearly measurable scintillation throughout, but there was no semblance of a geometrical enhancement as the line of sight scanned

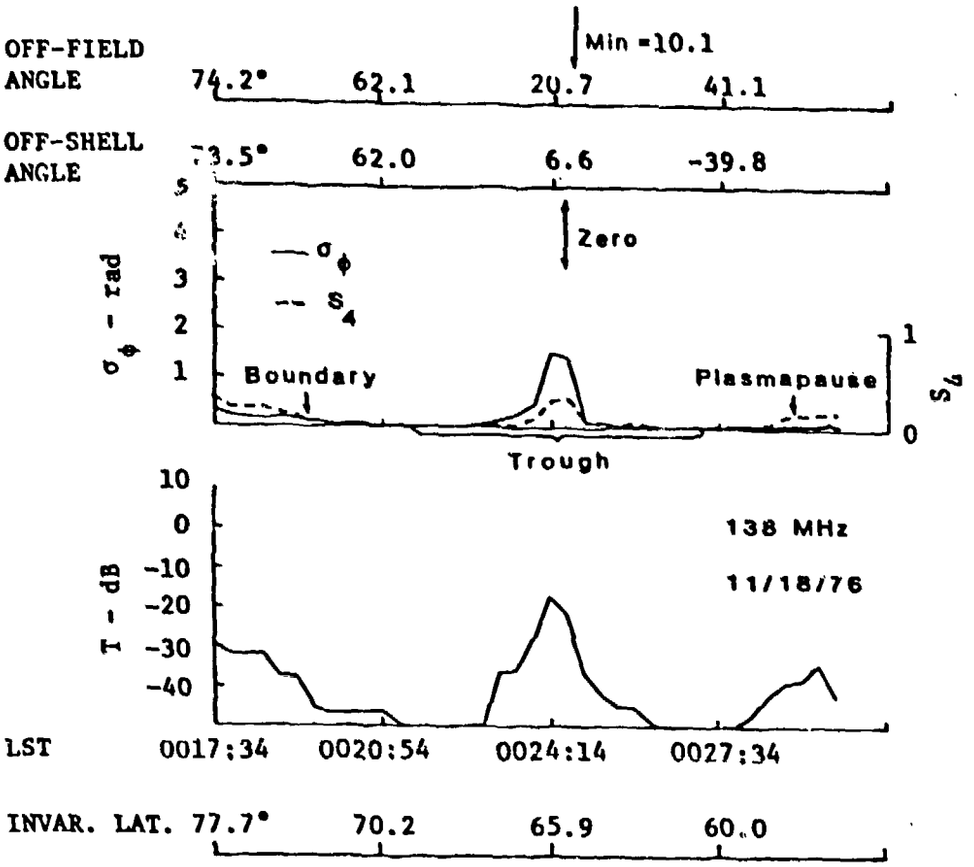

Figure 9. VHF scintillation indices (top) and phase PSD (bottom) for a nighttime overhead pass (essentially down the magnetic meridian) during which the boundary was poleward of the station. Note geometrical enhancement near the magnetic zenith (minimum off-field point).

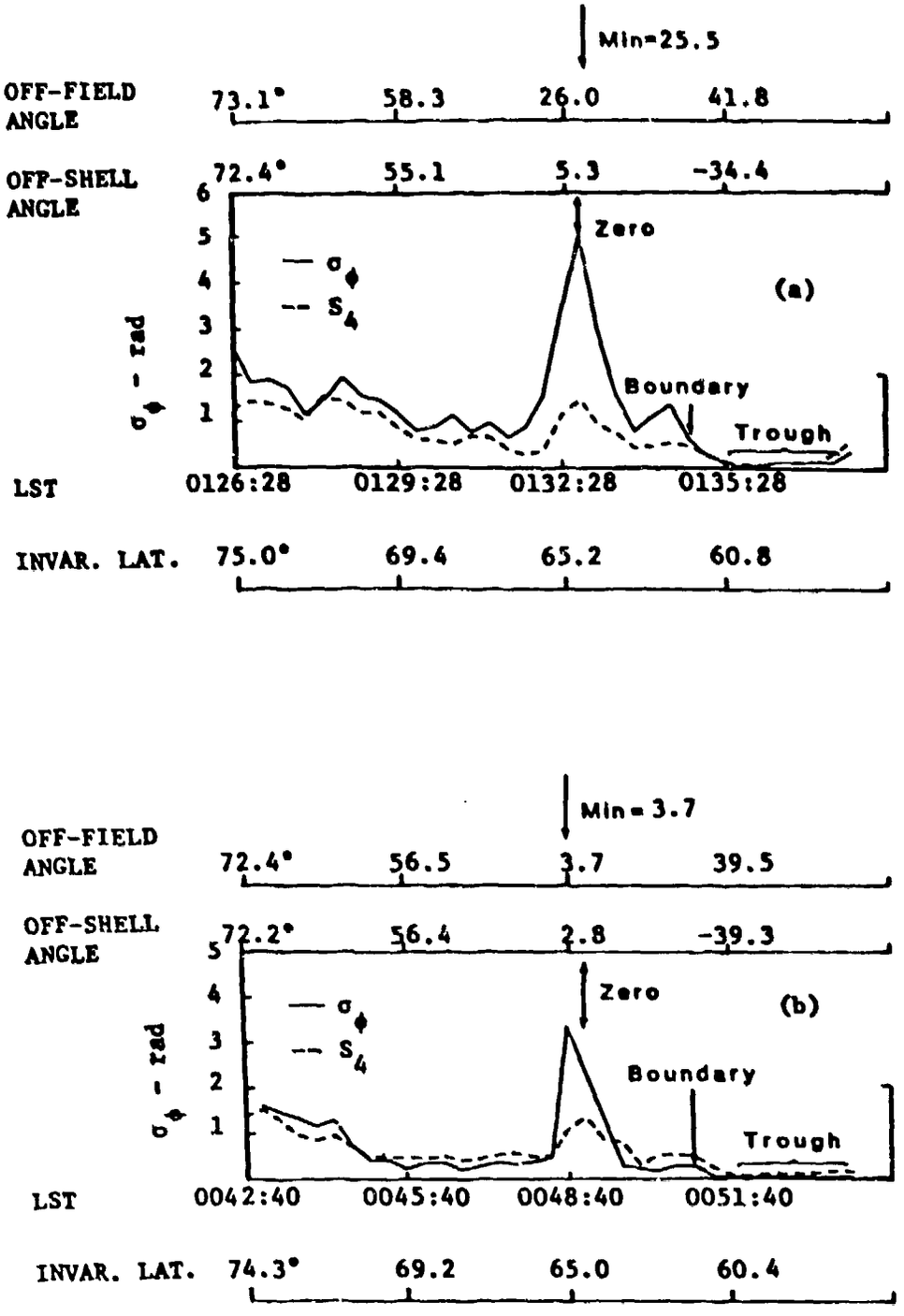

Figure 10. VHF (138-MHz) scintillation indices for two nighttime passes during which the boundary was equatorward of the station. Note strong geometrical enhancement in each at the point of grazing indicence to the L shell. (a) Off-meridian (nonoverhead) pass occurring on 8/18/78. (b) Overhead pass (essentially down the magnetic meridian) occurring on 1/30/79.

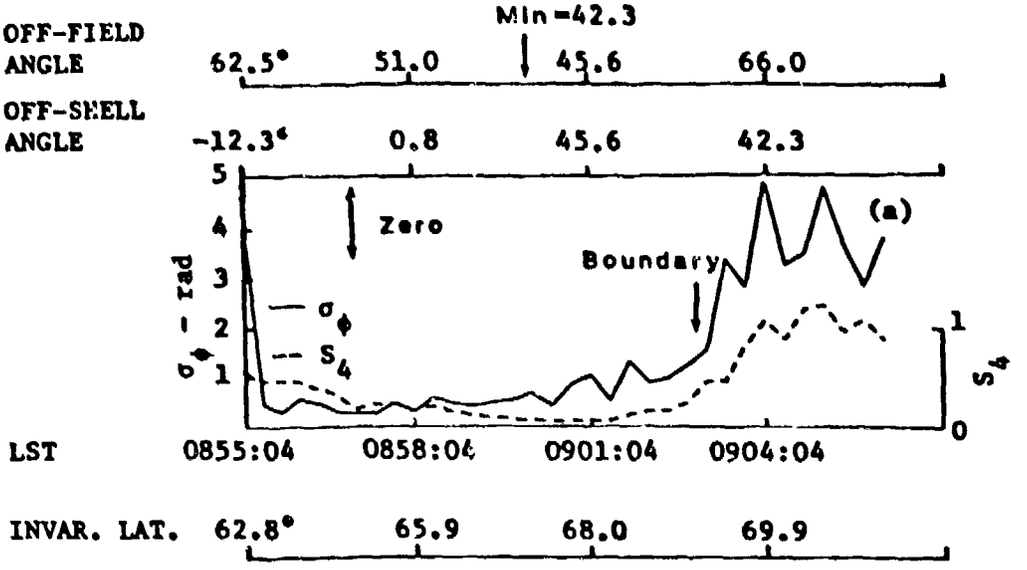

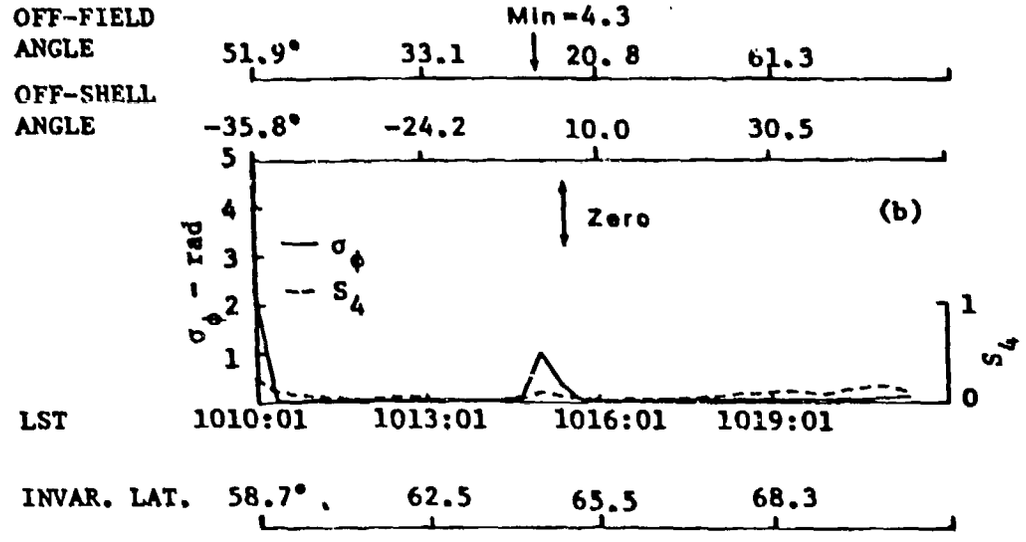

Figure 11. VHF scintillation indices for two daytime passes during which the boundary was poleward of the station. (a) Nonoverhead pass occurring on 12/5/78. Note absence of geometrical enhancement. (b) Overhead pass occurring on 11/7/77. Note geometrical enhancement. (Double-headed arrow marks minimum off-shell angle with accuracy greater than the one decimal place carried on the scale.)

through zero off-shell angle. The point at which one would expect a geometrical enhancement from sheetlike irregularities is at the point of zero off-shell angle, which is marked with a double-headed arrow. (Unlike nighttime passes, daytime passes have a considerable east-west velocity component, with the result that zero off-shell angle and minimum off-field angle are considerably separated in time during nonoverhead passes.)

Figure 11b illustrates starkly contrasting behavior in an overhead pass that took place under extremely quiet conditions (K_p=0+). Any sustained scintillation activity presumably was far to the north of the station. (Regarding possible activity in the far south, we point out that the first and last data points in a pass may be contaminated by ground reflections.) Under these extreme conditions, the "enhancing ability" of field-aligned geometry is strikingly evident. Just as we concluded from passes such as those shown in Figures 8 and 9 that nighttime trough irregularities are rodlike, so we conclude from passes such as those shown in Figure 11 that daytime irregularities equatorward of the scintillation boundary also are rodlike.

Now we turn to the situation that has been most difficult to document: that in which Poker Flat lies within the dayside high-latitude zone as defined by location of the scintillation boundary. Figure 12a shows a daytime pass quite far to the east of the station. For such passes, the satellite rises at a geomagnetic latitude only a few degrees equatorward of Poker Flat. The pass in question, P54-28, was moderately disturbed throughout, implying that the scintillation boundary lay equatorward of the pass start and decidedly equatorward of the station.

Taken at face value, lack of an enhancement in Pass 54-28 represents evidence that scintillation-producing irregularities on the day side of the high-latitude ionosphere are not sheetlike. Because the scintillation boundary was outside the window provided by the pass, however, one might question whether it sampled the high-latitude zone or trough irregularities. Figure 12b contains another example, in which the high-latitude scintillation is somewhat weaker but the boundary location more certain. This pass was to the west of the station, with a minimum off-field angle of 20.1°. The point of grazing incidence to the L shell was reached just poleward of the boundary, and no geometrical enhancement occurred. Figure 12c shows yet another example, in which the phase scintillation boundary was located at 59.4° invariant latitude. Again, there is no geometrical enhancement.

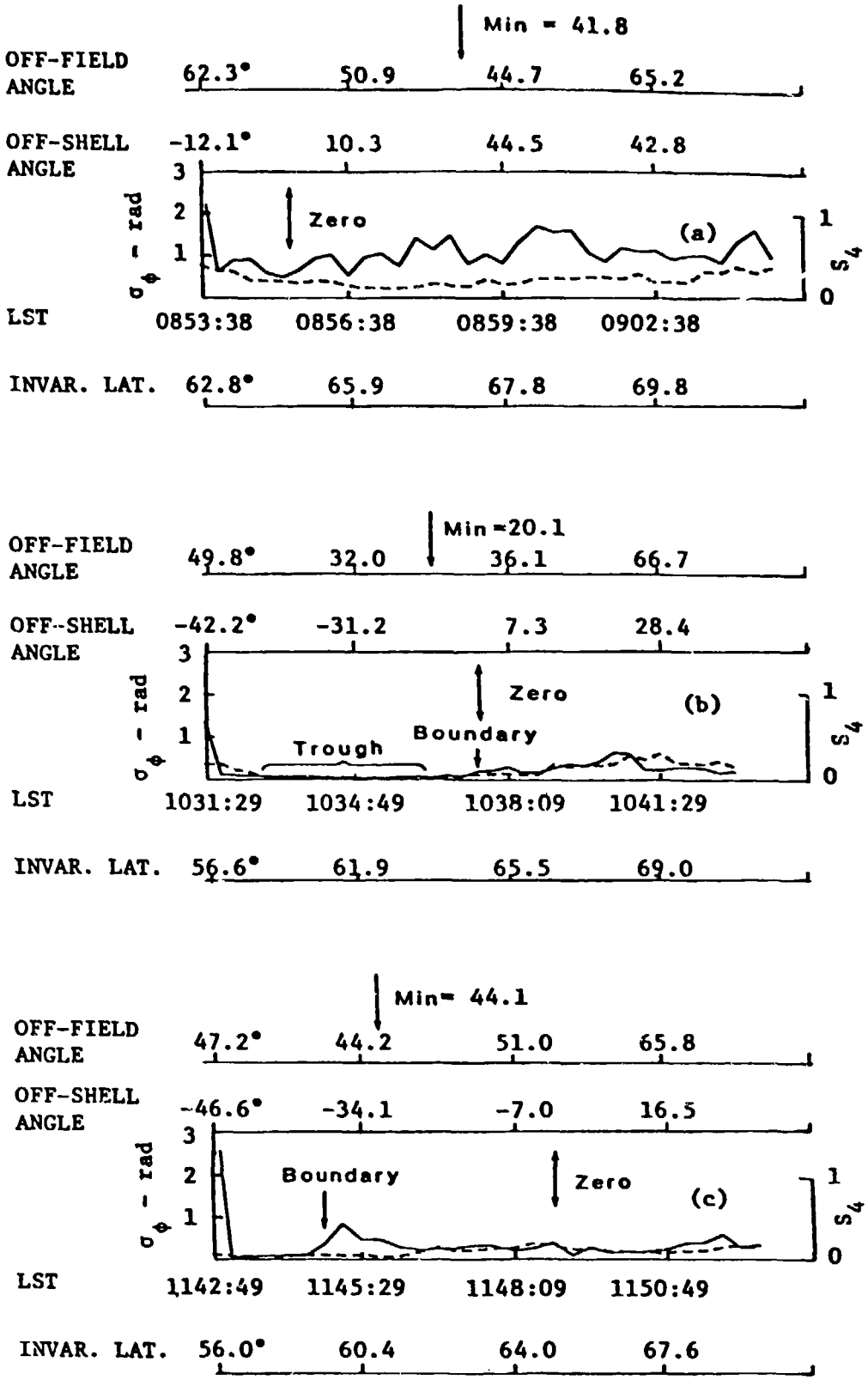

Figure 12. VHF scintillation indices for three nonoverhead daytime passes during which the boundary was equatorward of the station, occurring on (a) 8/11/78, (b) 2/2/77, and (c) 7/12/78. Note consistent absence of geometrical enhancement.

In contrast, Figures 13a and b show two nearly overhead daytime passes in which the scintillation boundary was located equatorward of Poker Flat. The minimum off-field angles were 3.3° and 2.6°, respectively, and the boundary latitudes are identified as 63.4° and 63.2°. There is no doubt that a geometrical enhancement occurred in both cases. The contrast between Figures 12 and 13, as well as between other nonoverhead and overhead passes, represents clear evidence that irregularities poleward of the dayside high-latitude scintillation boundary are rodlike rather than sheetlike.

We conclude from the behaviors illustrated in Figures 1 through 6, that (1) sheetlike irregularities are confined to the night side of the high-latitude ionosphere and (2) scintillation-producing irregularities in the other auroral-zone regions that we have addressed are rodlike. We have presented specific examples to illustrate the various behaviors, which we have found to be quite consistent in our Poker Flat data base, which numbers 1043 passes.

In conclusion (1) above, we use the term high latitude to mean poleward of the scintillation boundary. The latitude regimes with which we have dealt were established solely from the scintillation data, and although one might infer relationships with more fundamental ionospheric features (such as the plasmapause, the main trough, precipitation boundaries, and so forth), detailed relationships are apt to be complicated. Rino and Owen (1980) attempted to sort out some of the details by means of two-station scintillation and TEC observations. On the basis of their TEC analysis of three passes on a single night, they suggested that the nightside zone of sheetlike irregularities — or at least its source region — lies poleward of the diffuse auroral boundary. They did not make direct use of auroral data, however, and recognized the "severe limitations" of their TEC analysis technique, which does not yield a unique ionospheric description. Quite aside from the question of the precise latitudinal relationship of the various boundaries, however, incoherent-scatter observations by Vickrey *et al* (1980) corroborated salient features of the TEC-based inferences made by Rino and Owen (1980).

Supporting our conclusion that dayside irregularities are rodlike rather than sheetlike even poleward of the scintillation boundary is the fact that the behavior illustrated in Figures 5 and 6 is by no means unusual. We divided the 98 passes showing daytime scintillation boundaries equatorward of Poker Flat into six subgroups,

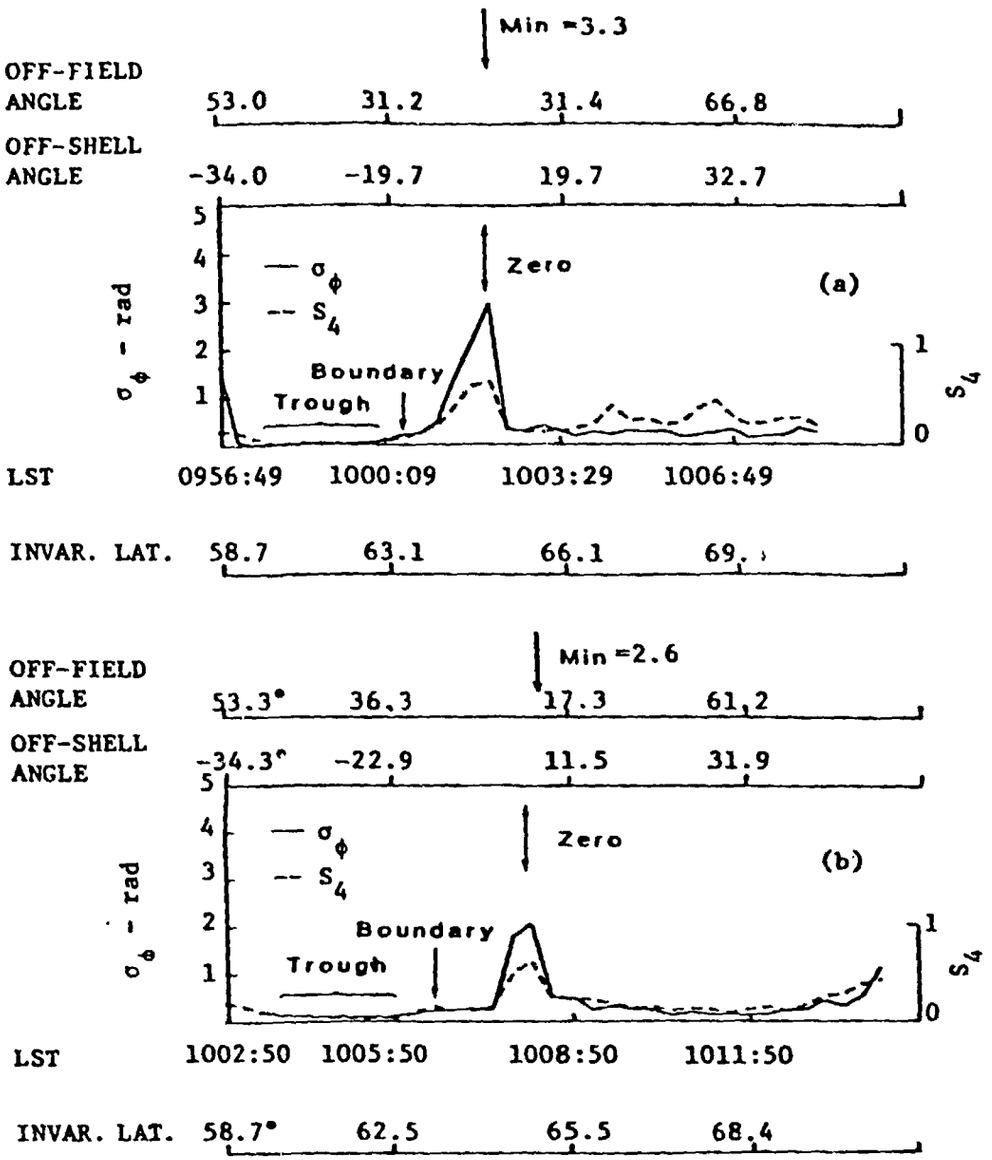

Figure 13. VHF scintillation indices for two overhead daytime passes during which the boundary was equatorward of the station, occurring on (a) 1/19/77 and (b) 12/11/77. Note geometrical enhancements near magnetic zenith in both.

depending upon the angular proximity to the station's magnetic zenith at the point of closest approach thereto. For instance, the near-overhead corridor contains 12 passes. Two corridors to the east of the station and three to the west also were defined, each containing a comparable number of passes.

Calculating the average value of σ_ϕ in each penetration-point latitude bin for the passes in each corridor, we found that only the overhead corridor displayed an appreciable geometric enhancement. Averaging a number of passes tends to smooth out latitudinal variations in height-integrated irregularity strength (the factor C_s in Equation 9) while retaining a persistent feature such as the geometrical enhancement. Figure 14 demonstrates the consistency of the difference between the overhead and nonoverhead passes.

Figure 14a shows the geomagnetic-latitude dependence of the average σ_ϕ values separately for the overhead pass corridor and for the 86 passes in the other five corridors. Both show higher values north of the station, which tends to be so in individual passes but which is accentuated somewhat on average by the latitude distribution of the boundary location. At the same time, they disclose quite measurable levels of scintillation to the south of the station.

The striking and important difference between the two curves in Figure 14a is the sharp maximum near 65° in the overhead corridor and the lack of any statistically significant peak there in the nonoverhead corridors. This difference is equally striking in Figure 14b, which shows the same two data sets plotted against off-shell angle of the line of sight rather than against geomagnetic latitude of the ionospheric penetration point. There is a resonance-like peak at zero off-shell angle for the overhead passes and none for the nonoverhead passes.

Just as we found a need for some circumspection in terminology regarding our conclusions about scintillation-producing irregularities on the night side, so we do on the day side. In speaking of the "high-latitude" ionosphere, we have addressed only those latitude regions observable from the receiving station at Poker Flat, which lies in the classical auroral zone. The station is ideally suited for investigating ionospheric conditions just poleward of and just equatorward of the high-latitude scintillation boundary, especially on the night side. Reliable extrapolation of results poleward and equatorward of $5 \leq L \leq 6$ would require data from other stations and/or other techniques.

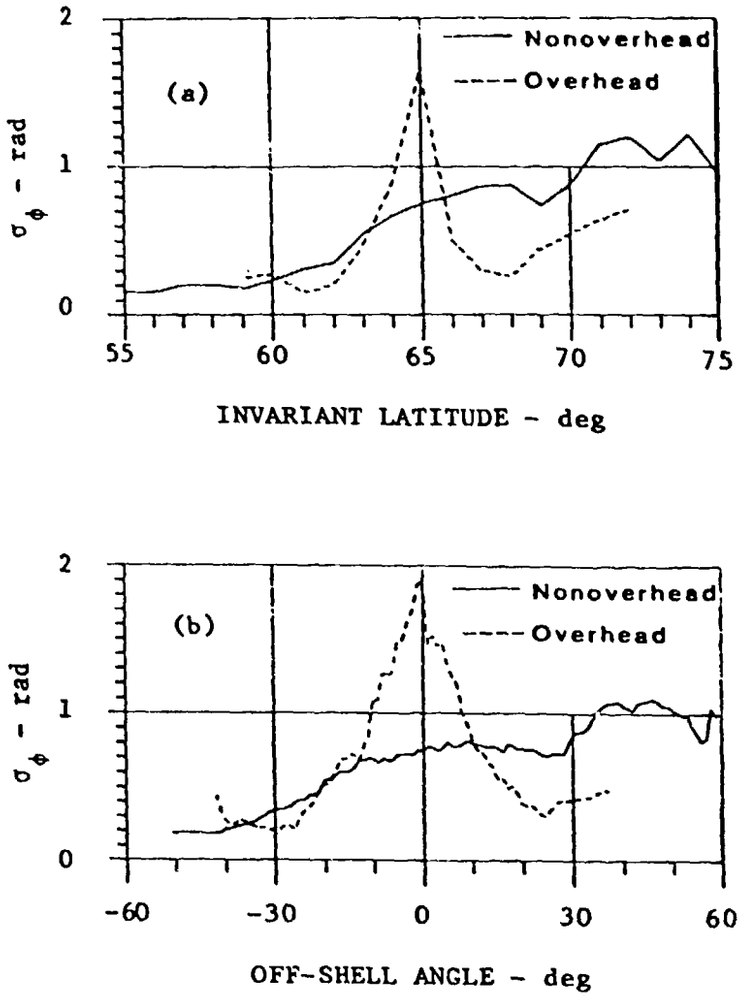

Figure 14. Average daytime VHF phase-scintillation index for 86 nonoverhead (solid) and 12 overhead (dashed) passes during which the scintillation boundary was equatorward of the station, displayed as functions of (a) invariant latitude of the line-of-sight penetration point and (b) angle between the line of sight and the local L shell, both calculated at an F-layer height of 350 km.

Within the above-stated limitations, Figure 14 demonstrates that rodlike behavior is the norm in the dayside high-latitude ionosphere. When we further restricted the data population to the passes in which the boundary location was judged more clear (79 of the 98 identified passes), the latitude and off-shell distributions changed very little. In the 86 nonoverhead daytime passes selected because the boundary could be identified as lying equatorward of Poker Flat, we found only five examples of scintillation enhancements that one might convincingly attribute to sheetlike irregularities. The counter examples revealed no preference for any particular state of magnetic disturbance, their average K being essentially the same as for the data population displaying the more common behavior.

D. Open Questions

Establishing qualitatively the dominant configuration of scintillation-producing irregularities probably is more important for sorting out source mechanisms than would be accurate determination of the axial ratios, a and b. Nonetheless, quantitative determination is desirable, and it would appear that one should be able to obtain reasonably accurate measurements by exploiting the geometrical enhancement predicted theoretically. Toward this end, in addition to dividing the 98 selected daytime passes into geometry corridors, we did so also for the overall daytime and nighttime populations.

Our approach was to calculate, for a given subset of passes, the average value of σ_ϕ in off-shell-angle bins, as was displayed in Figure 14b. As before, the individual σ_ϕ values were obtained from calculation of twenty-second standard deviations. The reason for averaging together a number of passes (having similar geometries) was to reduce the influence of individual scintillation patches -- in effect producing a kind of coherent averaging of the relatively stationary geometrical enhancement. After calculating the average values, we compared the results with values computed theoretically for a geometrical situation representative of the given data subset.

We found that a useful measure of the geometrical enhancement -- whether calculated or observed -- was its width in units of off-shell angle. Thus, we compared the observed enhancement widths with those calculated using different values of a and b. First, overhead passes were used to establish a, which turned out to be in the range

of 8 to 12, and then non-overhead passes were used to establish b, which was found to be about 4. Indeed, we have used values of 8 and 4 (and 1) respectively for a and b on the night (and day) side of the earth, respectively, in applications-oriented modeling.

The foregoing approach and results have provided the most reliable quantitative estimates available for irregularity axial ratios, for modeling of average scintillation (i.e., for representing expectation level in a multi-pass aggregate sense). We have found, however, that the results probably represent only a lower limit on the axial ratios, due to several factors that tend to broaden the enhancements observed in the data subsets.

The fundamental limitation to the approach is that the off-shell angle changes appreciably (between three and seven degrees, depending on the specific geometry) during a twenty-second period. Finer resolution would produce sharper observed enhancements. In addition, we have found that the precise location of the enhancement center varies from pass to pass. That is, it can occur slightly poleward or equatorward of the point at which the off-shell angle is zero. Thus, averaging together passes from a subset tends to broaden the enhancement further.

In light of the foregoing difficulties, we reverted to analysis of individual passes, using data processed to produce somewhat better resolution. For the purpose, we backed up from the summary tapes routinely obtained from SRI to tapes containing less highly processed data, namely time series of individual (albeit detrended) phase samples from 28 selected nighttime passes.

We calculated the standard deviation of phase over ten-second (rather than twenty-second) intervals, incremented each second (rather than each twenty seconds), and displayed them as finer-resolution plots vs. off-shell angle, as in Figure 15. We then applied a fifth-order least-squares fit to each observed curve, to introduce some smoothing, and compared the smooth curve to theoretically computed ones. The observed enhancement widths so determined correspond to substantially larger axial ratios (typically, exceeding 20 for both a and b on the night side) than those found in the analysis of aggregate subsets.

The very narrowness of the observed enhancement, unfortunately, renders any quantitative estimate of axial ratios based on its interpretation by means of a statistically homogeneous phase-screen model risky. This point is best appreciated, perhaps, by inspection of Figure 16, which shows the central portion of the phase

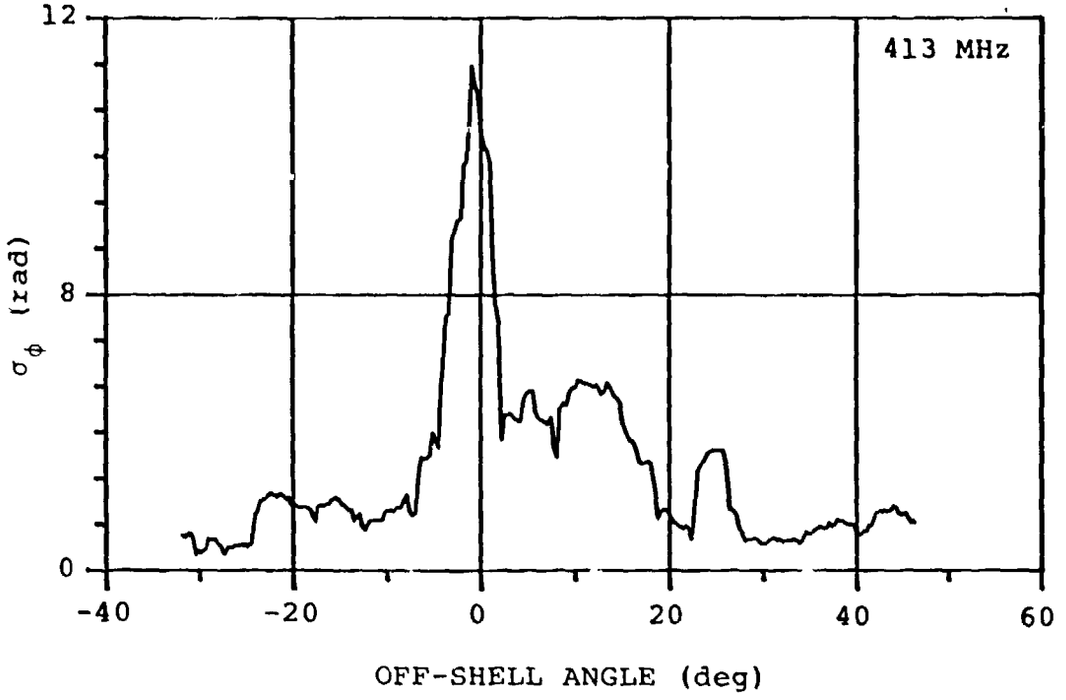

Figure 15. High-resolution plot of rms phase fluctuation through geometrical-enhancement region of Poker Flat Pass 61-33, which occurred on 29 January 1979 at about 0008 LST.

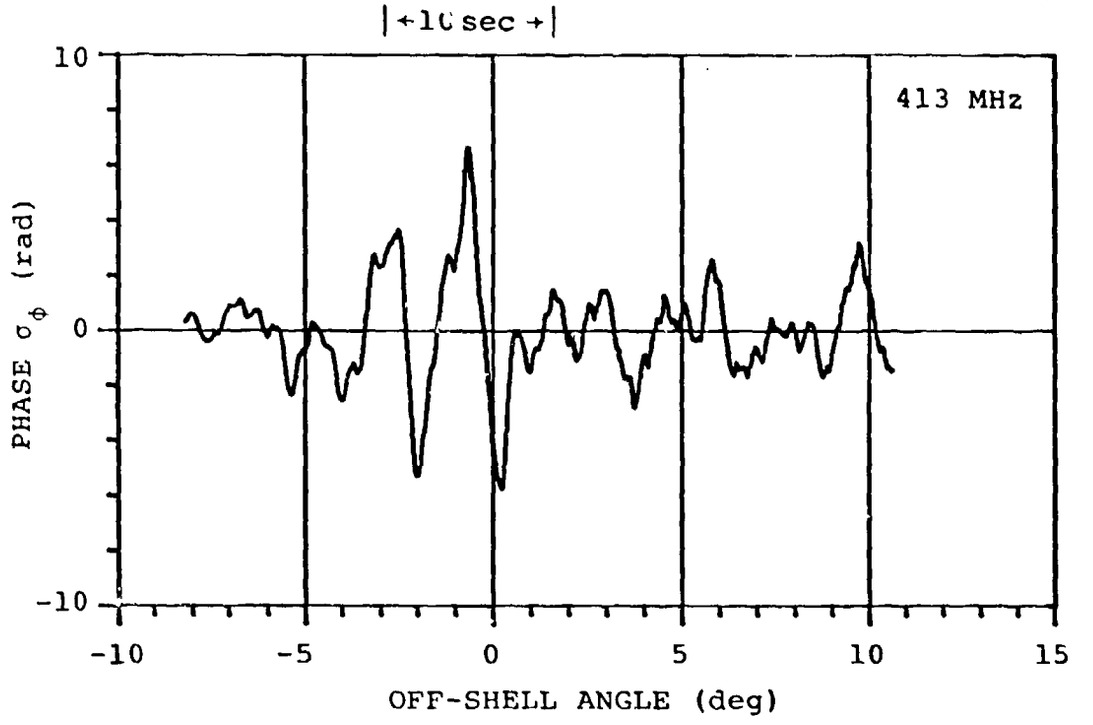

Figure 16. Portion of UHF phase record (plotted vs. off-shell angle) from which Figure 15 was calculated.

record from which Figure 15 was calculated. Two points are to be noted. First, the visually apparent enhanced phase variation persists for no more than ten seconds. Second, the enhancement clearly is dominated by large-scale structures, the dominant frequency of which places little more than two cycles within those ten seconds.

That the goemetrical enhancement is rich in low frequencies has been known for some time. For instance, Fremouw and Lansinger (1979) reported an increase from about 2.2 to about 2.5 in the power-law slope, p, of the phase spectrum in the enhancement region, for a large aggregate of data. Some individual passes, however, show a substantially larger value of p and a true dominance of the enhancement by large-scale structure. The effect is exemplified by Pass 61-33, and its phase spectrum in the enhancement region is shown in Figure 17.

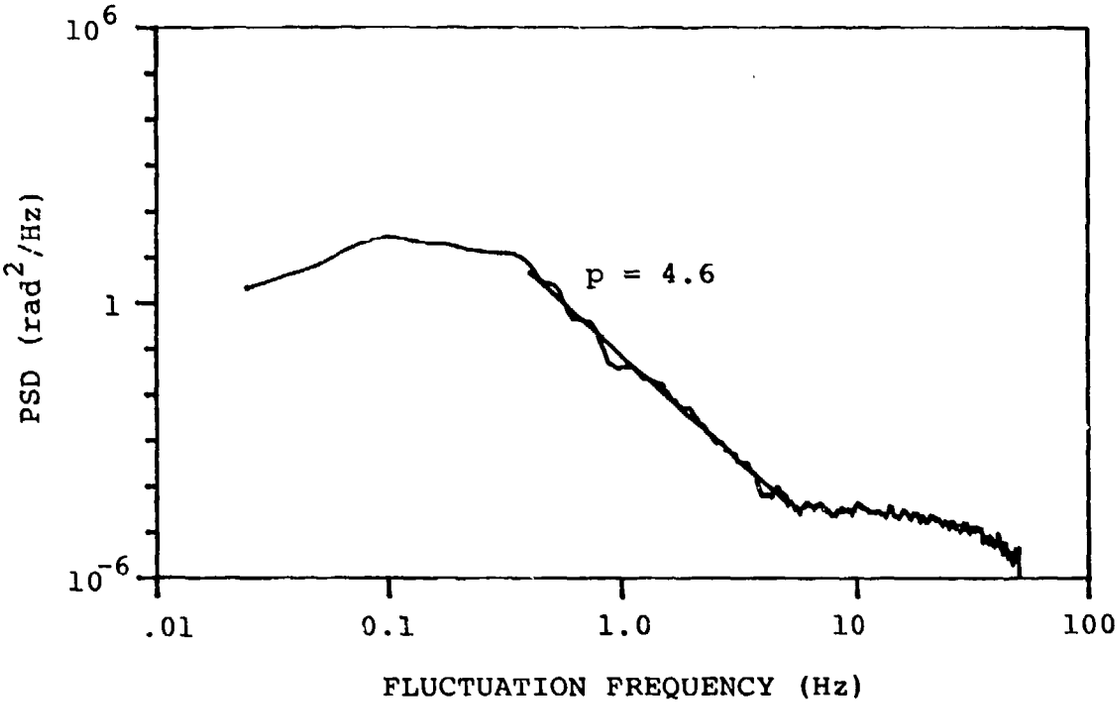

Figure 17. Power spectral density (PSD) of a 41-second portion of the phase record contained in Figure 16, including the geometrical enhancement. Straight line indicates best-fit power law, which has a spectral index of 4.6.

The spectrum rises from a noise floor of a little over 10^{-4} rad^2/Hz and follows a power law to a frequency somewhat higher than the 0.1-Hz cutoff imposed by the ten-second detrender. The straight line in Figure 17 represents a least-squares best fit in the power-law regime and yields a spectral index, p, of 4.6. It has not been determined whether this value of p relates directly to the irregularities or stems from the nonstationarity of the data (i.e., the little more than two cycles of enhanced low-frequency content). Whichever may turn out to be the case, it is clear that the enhancement is dominated by low frequencies more substantially than would be implied by an increase in p from 2.2 to 2.5.

The low-frequency dominance of the enhancement in this case, and in the small number of similar ones that have been analyzed, raises some new questions about the nature of the enhancement. There is little doubt that it is caused by L-shell-aligned sheetlike structures (on the night side). But it is now unclear whether, in fact, the sheets are identical with the power-law irregularities primarily responsible for scintillation when the line of sight is not nearly aligned with an L shell or not. Alternatively, they may represent a separate spectral class of larger structures in which the smaller ones are imbedded. One could, for instance, envision relatively large ionization sheets within which smaller rodlike irregularities reside.

In the latter view, the scintillation enhancement would arise from fortuitous propagation at small grazing angles to the large sheets, which might well be identical with the ionization "blobs" detected by Vickrey *et al* (1980) by means of incoherent scatter. To be sure, such large-scale structures would be unstable to the E x B and gradient-drift instabilities, as discussed by the latter authors. In the view put forth here, however, those instabilities would not have to produce L-shell-aligned secondary structures, which have yet to be clearly demonstrated in numerical simulation (Keskinen *et al*, 1980). We suggest that careful investigation of the spectral content of the geometrical enhancement might provide important clues to the dynamics of irregularity development. One aspect of such an investigation might be determination of a cross-field axial ratio, b, which is a function of spatial scale. An alternative description might be in terms of an *in-situ* spectrum with different power-law indices in different directions (i.e., a second kind of anisotropy).

Whatever the qualitative nature of the *in-situ* spectrum, it appears that quantitative determination of axial ratios from phase-scintillation enhancement at a single antenna requires considerable caution. Indeed, doing so on the basis of a theory founded on statistical homogeneity may not be possible. It may be necessary to employ spaced-receiver data, which in fact were collected in the Wideband experiment. As an example, we display phase-difference measurements from two pairs of spaced receivers in Figure 18.

The Wideband experiment included measurement at UHF receivers spaced several hundred meters apart along geomagnetic north-south and east-west baselines. Phase and intensity were measured at each receiving antenna, the former employing the same S-band reference used for the standard central-receiver VHF, UHF, and L-band measurements. Phase differences between antennas, then, represent measures of phase gradient along the baselines. Figure 18 displays such differences for the 413-MHz signals received at antennas spaced 900 meters apart north-south (top) and east-west (bottom). The records leave no doubt that the phase patterns on the ground were quite extended in the geomagnetic east-west direction throughout the time during which the line of sight scanned through small grazing angles to the local L shell.

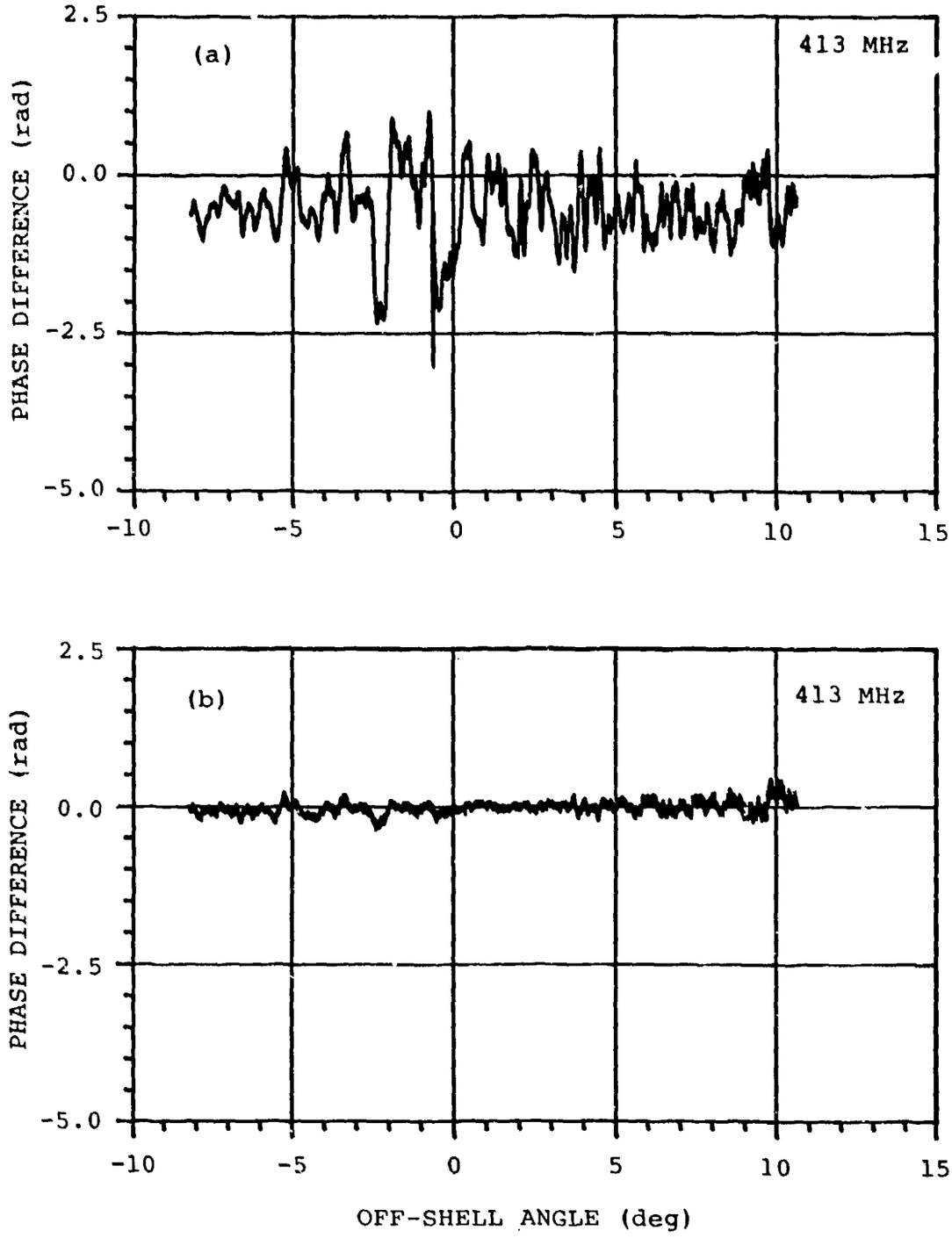

Figure 18. Phase difference between UHF signals received at antennas spaced 900 meters apart in (a) a geomagnetically north-south and (b) a geomagnetically east-west direction during Pass 61-33.

III. CONCLUSION

Work under this contract has contributed information about scintillation-producing irregularities in the auroral zone of two main types; occurrence trends and three-dimensional configuration. On the former topic, two main results were obtained. First, a quantitative relationship was found between solar activity, as measured by sunspot number and radio flux, and phase scintillation. It was found to be quite direct and to exist on time scales shorter than those included in annual means of the solar indices viewed as measures of epoch in an eleven-year activity cycle. Second, no statistically significant seasonal variation was found in scintillation activity in the Alaskan sector, in spite of a careful search of very high-quality data. This null result contrasts sharply with the strong seasonal variation found in the Greenland sector by Basu (1975).

Regarding the three-dimensional shape of auroral-zone irregularities, dominant configurations were established, difficulties were found with providing quantitative description of those configurations, and a new question regarding the nature of the irregularities has been posed. Scintillation-producing irregularities clearly are non-isotropic, and we explored their anisotropy in four regions: poleward and equatorward of the high-latitude scintillation boundary on the day and night sides of the earth.

We found that the irregularities display elongation along the magnetic field in all four regions and axial symmetry in three of them. Poleward of the boundary on the night side, we found three-dimensional anisotropy of the irregularities primarily responsible for phase scintillation. There, and only there, did we find the dominant configuration to be that of sheetlike structures layered like onion skins along magnetic L shells.

We employed statistical methods and phase-screen scattering theory to estimate axial ratios for describing (two- and three-dimensionally) anisotropic irregularities that would be consistent with aggregate subsets of scintillation data, given statistical homogeneity of the random medium. Our recent work has thrown open to question, however, the application of such estimates to description of irregularities on a case-by-case basis. While there is little doubt about the dominant configurations in a qualitative sense, describing them quantitatively by means of dimensional axial ratios

is less certain. The uncertainty stems from the short duration of the geometrical enhancements used to make the estimates as compared with the dominant Fourier periods contained in the enhancements. We suggest that direct use of spaced-receiver measurements may be more reliable than interpretation of single-receiver enhancements by means of statistically homogeneous phase-screen theory.

The dominance of the geometrical enhancement in phase scintillation by large-scale (low-frequency) structures raises a question about the nature of sheetlike irregularities. Models discussed in the literature until now have tacitly assumed three-dimensional isotropy of the spectral index employed to describe the *in-situ* power spectrum. It is probably true, however, that most researchers in the field would admit the possibility that this simplifying assumption might be violated. We suggest that the apparent scale-size dependence of geometrical enhancement may represent a situation in which such a violation occurs. An alternative description would be in terms of a cross-field axial ratio that varies with scale size.

A heuristic picture would be of large-scale sheetlike structures in which smaller-scale axially symmetric irregularities are imbedded. In this view, our results would indicate that the latter are present poleward of the high-latitude scintillation boundary on both the day and night sides of the earth (and, in a weaker state, equatorward of the boundary as well). The larger-scale sheets would be present, with few exceptions, only poleward of the boundary on the night side. The latter might well provide instabilities, but they would themselves represent a dynamical class apart from the former, having their own underlying generation mechanism. In particular, L-shell alignment would not depend upon extremely nonlinear development of convective instabilities as proposed by Ossakow and Chaturvedi (1979), Chaturvedi and Ossakow (1980), and Keskinen *et al* (1980).

Direct laydown by structured soft-electron precipitation is suggested as a candidate source of large-scale sheetlike structures in the F layer. In this work, we have found a very systematic relationship between the scintillation boundary and the soft-particle boundary reported by Gussenhaven *et al* (1981). Specifically, the two regions appear to be essentially co-located, except that the former is shifted poleward on the day side and equatorward on the night side relative to the latter. The picture that emerges is of irregularities developing within precipitation-produced plasma as it convects anti-sunward. The night-side shell-aligned structure would be a signature of

shell-aligned precipitation rather than of a convective instability, even though there would be subsequent interaction between the two.

It should be possible to test the foregoing conjecture and related ideas within the next few years. A key measurement will be of latitudinal structure in very soft ($\lesssim 100$ ev) electron precipitation in the nightside diffuse aurora simulataneously with measurement of structured total-electron content, phase scintillation, and anisotropic phase gradients associated with the latter. These measurements will be forthcoming in a multi-experiment satellite mission proposed to DNA by PD and now planned for launch in the second half of CY 1982 with participation by AFGL and other organizations.

Publications and Presentations

Results of this research have been reported in two published articles, one oral presentation at an international scientific meeting, and three oral presentations at national scientific meetings and were heavily drawn upon during participation by the Principal Investigator in an international workshop. These publications and presentations are listed below in chronological order, and abstracts appear on the immediately following pages.

Fremouw, E. J. and J. M. Lansinger, "Some Characteristics of Phase and Intensity Scintillation in Alaska," paper presented at National Radio Science Meeting (Spring URSI), University of Washington, Seattle, June 1979.

Fremouw, E. J., "On the Ratio of Intensity and Phase Scintillation Indices," paper presented at National Radio Science Meeting (Spring URSI), University of Washington, Seattle, June 1979.

Fremouw, E. J., "The Status of Scintillation Modeling," invited review paper presented at National Radio Science Meeting (Fall URSI), University of Colorado, Boulder, November 1979.

Fremouw, E. J., Contribution to "Transionospheric Propagation Predictions" compiled by J. Klobuchar in Solar-Terrestrial Predictions Proceedings, Vol. 2, ed. by R. F. Donnelly, Boulder, December 1979.

Fremouw, E. J., "Geometrical Control of the Ratio of Intensity and Phase Scintillation Indices," J. Atmos. Terr. Phys., 42, 775-782, 1980.

Fremouw, E. J. and J. M. Lansinger, "On the Three-dimensional Configuration of Scintillation-producing Irregularities in the Auroral Zone," paper presented at 4th Scientific Assembly of IAGA, Edinburgh University, August 1981.

Fremouw, E. J. and J. M. Lansinger, "Dominant Configurations of Scintillation-producing Irregularities in the Auroral Zone," J. Geophys. Res., 86 (A11), 1981.

SOME CHARACTERISTICS OF PHASE AND INTENSITY SCINTILLATION IN ALASKA

E. J. Fremouw and J. M. Lansinger
Physical Dynamics, Inc.
Bellevue, WA 98009

Abstract

The VHF (138 MHz) signal received at Poker Flat, Alaska, in the auroral zone (L = 5.5) from the Wideband coherent beacon on satellite P76-5 has been analyzed to determine morphological characteristics of complex-signal scintillation and of the ionospheric irregularities that produce it. Twenty-second values of the standard deviation, σ_ϕ, of VHF dispersive phase (measured relative to S Band) and of the normalized standard deviation, S_4, of VHF intensity (square of amplitude) are employed as scintillation indices. To date, results have been obtained from analysis of 21 months of data, collected from launch through February of 1978. Data from 697 satellite passes were selected by means of rather stringent data-quality criteria and have been sorted against a number of variables. The processed results have been interpreted in terms of a phase-screen scattering model containing a description of three-dimensionally anisotropic irregularities.

Initial results strongly support the idea that plasma-density irregularities in the auroral ionosphere (at least in the region of diffuse particle precipitation) characteristically take the form of sheets aligned along L shells rather than of axially symmetric rods. The results disclose, on the other hand, that irregularities in the daytime subauroral ionosphere are axially symmetric, elongated along the magnetic field. This difference causes the geometric behavior of the transionospheric communication channel at moderately high latidues to differ significantly between day and night.

Presented by J. M. Lansinger at National Radio Science Meeting, University of Washington, Seattle, June 1979.

ON THE RATIO OF INTENSITY AND PHASE SCINTILLATION INDICES

E. J. Fremouw
Physical Dynamics, Inc.
Bellevue, WA 98009

Abstract

Among the earliest characteristics of complex-signal scintillation noted from the DNA-002 Wideband Satellite Experiment (Fremouw *et al*, Rad. Sci., 13, 167-187, 1978) was a sizeable difference in the ratio of the intensity scintillation index, S_4, to the phase scintillation index, σ_ϕ, when measured at mid-latitude (Stanford), auroral-zone (Poker Flat), and equatorial (Ancon) stations. It has been found that two equatorial stations, Ancon and Kwajalein, consistently show a larger S_4/σ_ϕ ratio than does Poker Flat (Alaska), for conditions of nonsaturated intensity scintillation. Records from the aforementioned four receiving stations were carefully inspected to find data segments that show reasonable statistical stationarity over at least 20 sec (60 km of F-layer scan) and are well distributed in elevation angle and scintillation level. A plot of S_4 vs. σ_ϕ for 62 VHF data sets so selected shows essentially linear relationships up to a saturation regime beginning near $S_4 = 0.8$ and approaching $S_4 = 1.0$ asymptotically for three of the stations. Curves for the two equatorial stations coincide and display a decidedly steeper linear portion than that for the auroral-zone curve. The mid-latitude data points show much more scatter than do those from the other stations.

The phase-screen theory for production of scintillation in a power-law random medium has been reviewed to determine the relationship of the S_4/σ_ϕ ratio to properties of the medium in the non-saturated regime (weak to moderate intensity scintillation). It is possible to separate four factors as an aid to physical interpretation. In this paper, the behavior of two of the factors is explored for models describing both sheetlike and rodlike plasma-density irregularities. The analysis permits rejection of the effects of static diffraction by field-aligned irregularities (whether rodlike or sheetlike) at substantially the same altitude, as the factor controlling the different behaviors observed. It is shown, on the other hand, that geometrical control of the effective outer scale imposed by detrend filtering in the presence of highly anisotropic irregularities can readily explain the observed behavior.

It is concluded, further, that other factors may contrive to mitigate the effect of the controlling factor identified, which otherwise might produce even more marked difference in behavior at the various stations.

It is stressed that detrending effects are not to be viewed merely as experimental artifacts. Such effects arise in virtually all experiments and operational systems in the presence of a power-law spectrum with a very large outer scale, and they are important in controlling the quantitative relationship between phase and intensity scintillation.

Presented by E. J. Fremouw at National Radio Science Meeting, University of Washington, Seattle, June 1979.

THE STATUS OF SCINTILLATION MODELING

E. J. Fremouw
Physical Dynamics, Inc
Bellevue, WA 98009

Abstract

Among the modern objectives of ionospheric prediction is a desired capability to provide prior assessment of transionospheric propagation conditions. For transionospheric systems susceptible to group delay and dispersion, TEC predictions are of prime interest. For other communication systems, the main need is for assessment of scintillation conditions. A true predictive capability for scintillation has not yet been achieved, but descriptive scintillation models can provide a vehicle for implementing predictions on the basis of either large data bases of fundamental understanding of mechanisms (or, most likely, a combination of the two). Such models provide both signal-statistical characterization of complex-signal (both phase and intensity) scintillation and information on temporal and spatial occurrence trends (morphology). Scintillation models currently available, and being improved, are based on three data types: (1) past scintillation observations, (2) spread-F and other ground-based ionospheric records, and (3) *in-situ* measurements of electron-density irregularity. This paper will summarize the present status of scintillation models based on the forgoing three types of data base and on current understanding of scintillation production mechanisms.

Presented by E. J. Fremouw at National Radio Science Meeting, University of Colorado, Boulder, November 1979.

GEOMETRICAL CONTROL OF THE RATIO OF INTENSITY AND PHASE SCINTILLATION INDICES

E. J. Fremouw
Physical Dynamics, Inc.
Bellevue, WA 98009

Abstract

Early observations of complex-signal scintillation revealed a sizeable difference in the ratio of the intensity scintillation index, S_4, to the phase scintillation index, σ_ϕ, when measured at mid-latitude, auroral-zone, and equatorial stations. The differences observed between auroral and equatorial stations receiving a beacon signal from a polar-orbiting satellite have now been found to persist, for non-saturated values of S_4. The phase-screen theory for production of scintillation is employed in this paper to identify four factors that control the S_4/σ_ϕ ratio, and the behavior of two of them is explored for models describing both sheetlike and rodlike plasma-density irregularities. The analysis permits rejection of the effects of static diffraction by field-aligned irregularities (whether rodlike or sheetlike) as the factor controlling the different behaviors observed. It is shown, on the other hand, that geometrical control of the effective outer scale imposed by detrend filtering in the presence of highly anisotropic irregularities can readily explain the observed behavior. Such effects arise in virtually all experiments and radio systems operating in the presence of a power-law spectrum with a very large scale, and they are important in controlling the relationship between phase and intensity scintillation.

Published in J. Atmos. Terr. Phys., 42, 775-782, 1980.

ON THE THREE-DIMENSIONAL CONFIGURATION OF SCINTILLATION-PRODUCING IRREGULARITIES IN THE AURORAL ZONE

E. J. Fremouw and J. M. Lansinger
Physical Dynamics, Inc.
Bellevue, WA 98009, USA

Abstract

Phase scintillation observations have disclosed the existence of three-dimensionally anisotropic plasma-density irregularities in the auroral F layer. Taking the form of sheetlike structures aligned along L shells, these irregularities represent a dominant structure in the diffuse auroral region on the night side of the earth. The current-convective instability has been suggested as their source mechanism. In work reported here, we have exploited the aspect sensitivity of phase scintillation to identify the dominant three-dimensional configuration of irregularities in four latitude-time zones: (1) equatorward of the high-latitude scintillation boundary on the night side, (2) poleward of the nightside boundary, (3) equatorward of the boundary on the day side, and (4) poleward of the dayside boundary. We find consistent evidence that the sheetlike irregularities are confined to region (2), with few exceptions. The dominant configuration in the other zones, including (4), is that of axially symmetric rodlike irregularities aligned along the magnetic field. The disparity of three-dimensional configuration must be accounted for in theoretical understanding of irregularity source mechanisms.

Presented by E. J. Fremouw at 4th Scientific Assembly of IAGA, Edinburgh University, August 1981.

DOMINANT CONFIGURATIONS OF SCINTILLATION-PRODUCING IRREGULARITIES IN THE AURORAL ZONE

E. J. Fremouw and J. M. Lansinger
Physical Dynamics, Inc.
Bellevue, WA 98009

Abstract

Recent scintillation observations have disclosed the existence of sheetlike electron density irregularities aligned along L shells in the auroral-zone ionosphere. In this paper we exploit the aspect sensitivity of phase scintillation to identify the dominant three-dimensional configuration of irregularities in four latitude/time zones: (1) equatorward of the high-latitude scintillation boundary on the nightside of the earth, (2) poleward of the nightside boundary, (3) equatorward of the boundary on the day side, and (4) poleward of the dayside boundary. We find the sheetlike irregularities to be confined to region 2, with few exceptions. The dominant configuration in the other zones, including zone 4, is that of axially symmetric rodlike irregularities aligned along the magnetic field.

Published in J. Geophys. Res., 86 (A12), 1981.

GENERAL REFERENCES

Aarons, J. (1973), *A Descriptive Model of F Layer High-Latitude Irregularities as Shown by Scintillation Observations,"* J. Geophys. Res., 78, (31), 7441-7450.

Aarons, J., J. Mullen, and S. Basu (1964), *"The Statistics of Satellite Scintillations at a Subauroral Latitude,"* J. Geophys Res., 69, (9), 1785-1794.

Aarons, J., J. P. Mullen, and H. E. Whitney (1969), *"The Scintillation Boundary,"* J. Geophys. Res. 74 (3), 884-889.

Aarons, J., H. M. Silverman and B. A. Ramsey (1966), *"Latitudinal Effects on Satellite Scintillations,"* Ann. de. Geophys., 22, (3), 349-355.

Basu, Sunanda (1975), *"Universal Time Seasonal Variations of Auroral Zone Magnetic Activity and VHF Scintillation,"* J. Geophys Res., 80 (34), 4725-4728.

Basu, S. and S. Basu (1981), *"Modelling of Phase and Amplitude Scintillations at High Latitudes with AE-D Irregularity Data,"* paper presented at National Radio Science Meeting (Winter URSI), Boulder, CO

Boller, B.R. and H.L. Stolov (1970), *"Kelvin-Helmholtz Instability and the Semiannual Variation of Geomagnetic Activity,"* J. Geophys. Res., 75, 6073.

Booker, H. G., and J. A. Ratcliffe, and D. H. Shinn (1950), *"Diffraction from an Irregular Screen with Applications to Ionospheric Problems,"* Phil. Trans. Roy. Soc. Ser. A., 242, 579.

Briggs, B. H., and I. A. Parkin (1963), *"On the Variation of Radio Star and Satellite Scintillations with Zenith Angle,"* J. Atmos. Terr. Phys., 25 (6), 339-366.

Chaturvedi, P. K. and S. L. Ossakow (1980), *"The Current Convective Instability As Applied To the Auroral Ionosphere,"* NRL Memorandum Report 4415, Naval Research Laboratory, Washington, DC.

Fejer, B. G., and M. C. Kelley (1980), *"Ionospheric Irregularities,"* Rev. Geophys. and Space Phys., 18 (2).

Fremouw, E. J. (1978), *"Analysis of Wideband Satellite Data,"* Bimonthly Progress Report No. 3, Contract DNA001-78-C-0042, Physical Dynamics, Inc., Bellevue, WA.

Fremouw, E. J., R. L. Leadabrand, R. C. Livingston, M. D. Cousins, C. L. Rino, B. C. Fair, and R. A. Long (1978), *"Early Results from the DNA Wideband Satellite Experiment —Complex-Signal Scintillation,"* Rad. Sci., 13 (1), 167-187.

Fremouw, E. J. and J. M. Lansinger (1979), *"Continued Geophysical Analysis of Coherent Satellite Scintillation Data,"* PD-NW-79-213R, Annual Report, Contract F49620-78-C-0014, Physical Dynamics, Inc., Bellevue, WA.

Fremouw, E. J. and J. M. Lansinger (1981), *"A Computer Model for High-Latitude Phase Scintillation Based on Wideband Satellite Data from Poker Flat,"* PD-NW--81-240R, Draft Final Report on Contract DNA001-79-C-0372, Physical Dynamics, Inc. Bellevue, WA.

Gussenhoven, M. S., D. A. Hardy and W. J. Burke (1981), *"DMSP/F2 Electron Observations of Equatorward Auroral Boundaries and Their Relationship to Magnetospheric Electric Fields,"* J. Geophys. Res., 86, (A2).

Ishimaru, A. (ed) (1975), *"Special Issue: Waves in Random Media,"* Rad. Sci., 10, (1).

Keskinen, M. J., S. L. Ossakow, and B. E. McDonald (1980), *"Nonlinear Evolution of Diffuse Auroral, F-Region, Ionospheric Irregularities,"* Geophys. Res. Ltrs., 8, 573.

Linson, L. M., and J. B. Workman (1970), *"Formation of Striations in Ionospheric Plasma Clouds,"* J. Geophys. Res., 75, 3211.

Livingston, R. C., C. L. Rino, J. P. McClure, and W. B. Hanson, *Spectral Characteristics of Medium-Scale Equatorial F-Region Irregularities*, J. Geophys. Res., 86 (A4), 2421-2428, 1981.

Meng, C.I. and S. I. Akasofu (1968), *"Polar Magnetic Substorms in the Conjugate Areas,"* Rad. Sci., 3, 751.

Ossakow, S. L. and P. K. Chaturvedi (1979), *"Current Convective Instability in the Diffuse Aurora,"* Geophys. Res. Ltrs., 6, 332.

Rino, C. L. and E. J. Fremouw (1977), *The Angle Dependence of Singly Scattered Wavefields*, J. Atmos. and Terr. Phys., 39, 859.

Rino, C. L. and S. J. Matthews (1978), *"On the Interpretation of Ionospheric Scintillation Data Using a Power-Law Phase Screen Model — Weak Scatter,"* Tech. Report 2, SRI Project 6434, Contract DNA001-77-C-0220, SRI International, Menlo Park, CA.

Rino, C. L. and J. Owen (1980), *"The Structure of Localized Nighttime Auroral Zone Scintillation Enhancements,"* J. Geophys. Res., 85 (A6), 2941-2948.

Rino, C. L. (1979a), *"A Power Law Phase Screen Model for Ionospheric Scintillation. 1. Weak Scatter,"* Rad. Sci., 14 (6), 1135.

Rino, C. L. (1979b), *"A Power Law Phase Screen Model for Ionospheric Scintillation. 2. Strong Scatter,"* Rad. Sci., 14 (6), 1147.

Singleton, D. G. (1970), *"Dependence of Satellite Scintillations on Zenith Angle and Azimuth,"* J. Atmos. Terr. Phys., 32, 789-803.

Vickrey, J. F., C. L. Rino, and T. A. Potemra (1980), *"Chatanika/Triad Observations of Unstable Ionization Enhancements in the Auroral F-Region,"* Geophys. Res. Ltrs., 1(10), 789-792.

Yeh, K.C., and C. H. Liu (1981), *"Radio Wave Scintillations in the Ionosphere,"* Invited for publication in IEEE during 1982.